Spring 5-2019

Development of a Multi-Probe Kelvin Scanner Device for Industrially-Relevant Characterization of Surface-Activated Carbon Fiber Reinforced Thermoplastic Composites

Kirby Simon
Washington University in St. Louis

Washington University in St. Louis

McKelvey School of Engineering

Department of Mechanical Engineering and Materials Science

Thesis Examination Committee:
Dr. Elijah Thimsen, Chair
Dr. Guy Genin
Dr. Patricia Weisensee

Development of a Multi-Probe Kelvin Scanner Device for Industrially-Relevant Characterization of Surface-Activated Carbon Fiber Reinforced Thermoplastic Composites

by

Kirby Simon

A thesis presented to the McKelvey School of Engineering
of Washington University in partial fulfillment of the
requirements for the degree of

Master of Science

May 2019
Saint Louis, Missouri

Acknowledgments

I would like to acknowledge Dr. Elijah Thimsen for his support throughout the duration of this project as well as my undergraduate research project in his lab. I would also like to say thank you to the other graduate students in the Interface Research Group for their help and support over the years.

My thesis is dedicated to my parents, family, and friends for helping me get to where I am now, encouraging and motivating me along the way.

Kirby Simon

Washington University in Saint Louis
May 2019

Contents

List of Tables

List of Figures

List of Abbreviations

CFRTP Carbon-Fiber Reinforced Thermoplastic

KPFM Kelvin Probe Force Microscopy

MPKS Multi-Probe Kelvin Scanner

RSS Root Sum Squared

SP Surface Potential

ABSTRACT OF THE THESIS

Development of a Multi-Probe Kelvin Scanner Device for Industrially-Relevant Characterization of Surface-Activated Carbon Fiber Reinforced Thermoplastic Composites

by

Kirby Simon

Master of Science in Materials Science and Engineering

Washington University in St. Louis, May 2019

Research Advisor: Dr. Elijah Thimsen

Carbon fiber reinforced thermoplastic (CFRTP) composites are becoming increasingly attractive materials in manufacturing due to their lightweight nature, mechanical strength, and corrosion resistance. Surface activation of these materials is usually required during processing to increase the bond strength of assemblies (aerospace and automotive industries) or improve adhesion with implants (biomedical industry). Industrially-relevant, non-destructive quality control methods for assessing the activation state of these materials do not currently exist, however. Applying principles discovered through the use of scanning probe microscopy, a multiple-probe Kelvin scanning (MPKS) device has been developed that can assess the uniformity of the activation state of plasma-treated CFRTP surfaces. The device can distinguish between control and plasma-treated samples and its measurements have been correlated with shear bond strength of epoxy-bonded assemblies. With the multiple probes increasing measurement speed, the automated device can be scaled for use in manufacturing-relevant environments and improve upon current quality control practices.

Chapter 1

Background

Carbon fiber reinforced thermoplastic (CFRTP) materials are becoming commonplace in manufacturing industries, such as the aerospace, automotive, and biomedical industries. For example, the Boeing 787 is now built of over 50% w.t. carbon fiber reinforced thermoplastic and thermoset materials [8]. Although thermosets have traditionally been used in aircraft assembly, thermoplastics are emerging as the favorable carbon fiber reinforced composite material used in these industries due to its ease of processing. Thermoplastics offer reduced raw materials and processing costs compared to epoxies used in thermosets [6, 11]. Along with this, raw materials for thermosets have a limited shelf life on the order of six months and must be stored in a refrigerator or freezer whereas the prepreg materials used to produce thermoplastics have an indefinite shelf life and can be stored in ambient conditions [5, 6]. Finally, crosslinked thermoset materials have limited recyclability while thermoplastic scraps can be pelletized and reused in the manufacturing process [6]. These production advantages, combined with improved damage tolerance [6, 11, 17], make carbon fiber reinforced thermoplastics a desirable material for use in assembly or repair of large structures such as aircraft and automobiles.

Before implementing these materials into manufacturing, however, surface activation steps are usually undertaken to prepare the materials for processing. In the aerospace industry, surface activation before bonding materials improves the resulting bond strength of the assembly [10, 12, 19]. This is beneficial in aircraft and automotive assembly and repair, where traditional welding or fastening methods used for metals are ill-suited for CFRTPs since welding or drilling holes through the material could denature or weaken the composite, although innovations in this area have led to new welding and bonding techniques [5, 11]. In

the biomedical industry, surface activation has the ability to disinfect the surface by killing bacteria or improve biocompatibility by altering the hydrophilicity of the material surface and thus tuning adhesion of proteins that facilitate colonization of the surface by host cells [4, 7, 16, 20]. Because of the necessity of these surface activation steps to integrating CFRTPs into manufacturing, it is of paramount importance to develop quality control methods to assess the material activation state. Quality control methods need to accurately characterize a surface to ensure that it has been properly activated, by plasma-treatment or some other form of surface activation, before using the material in assembly of structures or inserting the material into the body. Quality control instrumentation should allow for the non-destructive, non-wasteful assessment of the activation state of CFRTP material surfaces such that a device operator can make a go/no-go decision on the material in question in a manufacturing-relevant environment.

1.1 CFRTPs

CFRTPs are polymeric materials embedded with carbon fiber strands. Although CFRTP may refer to thermoset (amorphous, cross-linked) polymers along with thermoplastic (semi-crystalline, uncross-linked) polymers, this study was performed solely on thermoplastic materials and shall therefore be referred to as defined in the List of Abbreviations above. Thermoplastics were investigated in this study due to the advantages they provide over thermosets, as discussed above, and their emergence as an important material in the aerospace industry used for aircraft assembly and repair.

The two components of CFRTPs, the matrix and the fibers, have specific properties that contribute to the overall function of the material. The thermoplastic matrix serves as a continuous phase that holds the fibers in place. It fills the space between the fibers and transfers loads from fiber to fiber. Matrix materials should have a high adhesive strength to hold the fibers in place and be resistant to heat, chemicals, and moisture. The fibers, on the other hand, provide strength and stiffness to the material. Carbon fibers are commonly used in fiber-reinforced composites due to their low density, low coefficient of thermal expansion, high fatigue resistance, and electrical conductivity. The orientation of these fibers within the matrix can further impact the resulting composite properties. The fibers can be continuous

or discontinuous, laced or woven, and unidirectional or multidirectional, among other things. The orientation of the fibers varies from material-to-material depending on the anticipated mechanical load. Examples of CFRTP materials with different fiber layouts and orientations are displayed in Figure 1.1 below. Understanding the orientation of the fibers is crucial to determining the structural integrity of the composite and how the material will respond to different stresses.

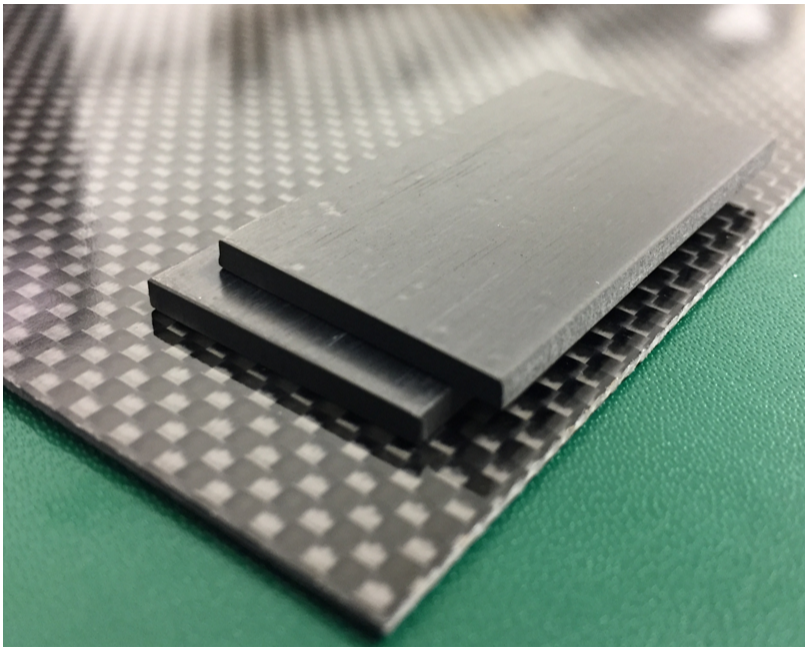

Figure 1.1: Examples of CFRTP materials with unidirectional and woven fiber orientations.

CFRTPs and other composite materials are becoming increasingly popular in manufacturing environments due to their performance improvements and ability to reduce the wholistic cost of manufacturing assemblies [6, 11]. Implementing these materials can decrease the weight of resulting structures while maintaining, and even improving, the structural integrity of the assembly [6, 11, 18]. This is beneficial in the aerospace and automotive industries, since decreasing the weight of aircraft or automobiles would drastically decrease fuel costs associated with transportation or allow more payload to be carried. Along with this, the corrosion resistance and thermal stability of these materials makes the resulting structures more resilient in inclement weather or harsh climates [18]. Finally, by implementing alternative bonding and assembling techniques that do not require mechanical fastening, fewer parts (i.e. fasteners,

screws) are utilized during assembly which reduces the cost and time needed to manufacture structures from composite materials such as CFRTPs [6, 11].

1.2 Surface Activation and Assembly

When assembling parts from thermoset and thermoplastic materials, common practice has involved either mechanically fastening or welding structures together [5, 17]. However, these processes serve as areas for concern with composites because mechanical fastening involves drilling holes through the composites, which weakens the material and can lead to corrosion at the interface between the composite and the metal fastener [5, 14], and welding requires high temperatures that can damage or denature the composite if not well-controlled. For these reasons, adhesive bonding of composites has been investigated as an alternative method for joining materials together into structures and assemblies. This practice involves applying an epoxy to two different composite surfaces and gluing them together. Heat and/or pressure are usually applied to the materials once they are in contact to accelerate the cure of the epoxy. The benefits of adhesive bonding, including the reduction of stress concentrators (since no holes are drilled through the material) and of the weight of the joint/bond (since no fasteners or screws are needed), make it a competitive alternative to traditional fastening or welding methods used for composite materials.

Bonding composite materials together without doing any surface preparation, however, does not always result in a strong bond. Therefore, various surface preparation techniques have been developed to improve the bond strength of assembled structures, namely mechanical roughening and peel ply techniques [23, 24]. Mechanical roughening is often done in the form of sanding or abrasion of the material surface, and although this technique increases the surface roughness of the material and facilitates interlocking of two materials when bonded together, there are significant downsides to this technique. It is difficult to ensure a surface is contamination-free post-treatment, as particulate matter from the composite or sanding material can easily be stuck to and in the roughened composite surface [24]. Along with this, damage can be done to the underlying fibers or matrix material if the sanding or abrasion penetrates too-deeply into the surface [24]. These problems with mechanical roughening result in variability of the bond strength epoxy-bonded composite materials, as

inconsistencies due to contamination or damage to the underlying composite can actually weaken the resulting bond.

Peel ply techniques involve co-curing a material to a composite surface and peeling the material away immediately before bonding, leaving behind a fresh surface at the bonding interface [24]. Although this technique is used in the aerospace industry when bonding structures, it also runs into issues with contamination from leftover peel ply material remaining on the surface [24]. Along with this, the peel plies typically absorb moisture and can therefore dry out the matrix at the bonding interface, which could further reduce the bond strength of the resulting assembly [24].

For these reasons, new surface preparation techniques are being developed that can more-reliably produce strong adhesive bonds between composite materials. Plasma-treatment is one of these emerging techniques, and it has been gaining traction in the aerospace industry as it has been proven to produce stronger bonded composite assemblies (i.e. stronger bonds between composite materials) than the traditional surface preparation techniques discussed above [22, 23, 24]. This processing technique involves generating a plasma in close proximity to a material surface such that the high-energy ions and electrons of the plasma interact with the material surface. These ions both etch and react with the material surface, chemically modifying the surface through functionalization and/or the generation and immobilization of free radicals while also generating surface roughness that can improve adhesion. This process creates a surface that is physically and chemically different from the pre-treated material surface. Producing this activated or "excited" surface state alters interfacial interactions between the material and its environment. For example, the traditionally hydrophobic CFRTP material surface becomes hydrophilic through plasma-treatment. This plasma-activated surface results in an increased bond strength of a resulting assembly or structure, making this technique a favorable practice in the aerospace and automotive industries [22, 23, 24].

Due to the importance of the surface activation step in CFRTP composite processing in the aerospace, automotive, and biomedical industries, it is vital to be able to assess the surface activation state of these materials prior to further processing to determine if the plasma-treatment (or other modification technique) was performed correctly. Quality control is therefore an important step in reliably assessing the activation state of CFRTP materials to

ensure that they have been adequately prepared for further processing and/or assembling of final products.

1.3 Quality Control Methods

Common quality control measures used in the aerospace and automotive industries for adhesive bonds between composites involve randomly sampling materials from the manufacturing line, performing destructive, mechanical tests on those materials (e.g. bonding followed by lap shear or compression testing), and then doing a statistical analysis on the results to determine the probability that the remaining materials were adequately prepared. This methodology is widely used in various manufacturing industries with high degrees of success, however there are several key issues with this method. First, since only a small representative number of materials are tested out of the entire population, there can be situations where ill-prepared materials slip through the cracks. In the automotive, aerospace, and biomedical industries, this is incredibly problematic as it could result in the malfunction of aircraft or automobiles during operation or increase the chance of infection in a patient, endangering the life of the end-users.

Along with this, mechanical testing and statistical analysis is ill-suited for custom jobs or repair operations. For example, if a single custom part is being produced or a hole in an aircraft is being repaired with a bonded composite, destructive testing and statistical analysis cannot be performed on the part since there are no duplicate parts to test and compare.

Finally, this procedure is destructive and therefore wasteful. Although CFRTP materials have the benefit over thermoset composites in that they are cheaper to manufacture and can be recycled for reuse [6], composite materials are still more expensive to produce than many aluminum parts so material losses should be minimized if possible.

Although destructive testing and statistical analysis has been used for years in manufacturing industries, there is a push to develop non-destructive testing methods that can accurately predict the bond strength of assemblies a) before bonding is performed and b) without destroying the resulting assembly. As surface-activation techniques are necessary to improve the bond strength of assemblies, it is therefore vital to understand and non-destructively

assess the surface of plasma-treated (or otherwise activated) materials to predict the bond strength of a resulting assembly before bonding is performed. Quality control methods should, therefore, assess the activation state of a prepared CFRTP composite material before and after treatment to allow the operator to determine if the material was adequately activated and will produce a strong bond in the resulting assembly.

Several methods exist for assessing surface activation states of materials that could potentially serve as quality control measures for CFRTPs and composites. These methods include contact angle measurements, scanning probe force microscopy, and material sampling coupled with statistical analysis (as discussed above). Contact angle measurements involve dropping water (or other polar and/or nonpolar liquids) on the sample surface and measuring the wettability of the surface as determined by the interaction at the liquid-solid interface. Scanning probe force microscopy, specifically atomic-force microscopy (AFM) and Kelvin probe force microscopy (KPFM), involves scanning a fine-tipped probe across the sample surface to map topography and assess surface activation through measuring the electrostatic force experienced by the probe when scanned at a constant tip-to-sample distance. These measurements are very sensitive to vibrations, electromagnetic interference, and variations in ambient conditions, such as changes in relative humidity and temperature [1, 3, 9, 21].

Although these practices are widely implemented in manufacturing and laboratory environments, they do not meet the needs of assessing surface-activated CFRTPs in the aerospace, automotive, and biomedical industries. This is because these quality control methods are, in general, destructive (to either the activation state or directly to the material), not suitable for assessing larger or non-uniform surfaces, and/or too sensitive to be implemented in manufacturing environments. The main issues with the quality control practices discussed above are summarized below in Table 1.1.

Table 1.1: Summary of Quality Control Methods for Assessing Surface-Activation

Method	**Challenge**
Contact Angle	Destructive; Not Effective for Rough Surface
Scanning Force Microscopy	Not Suited for Manufacturing Environments
Sampling & Statistical Analysis	Destructive; Ill-Suited for Custom/Repair Operations

Contact angle is a common method for assessing the surface activation state of materials and is marketed as a non-destructive quality control tool for various manufacturing environments. However, there are still shortcomings of this method with respect to assessing CFRTP and other composite materials. For example, depending on the liquid used to perform contact angle measurements, the activation state of the material surface may be damaged as the functional groups and radical species on the activated surface may undergo chemical reactions with the contacting liquid. For this reason, ultra-pure water is frequently used as the contacting liquid when performing contact angle measurements.

Contact angle measurements also suffer when there are surface deformities and irregularities present in the material. Since contact angle measures the wettability of a surface as a drop of liquid spreads out on the material surface, any obstructions or deformities along the sample surface may disrupt the ability of the liquid to spread and give an inaccurate measurement. An example of this instance is seen in Figure 1.2 below, where a small amount of deionized water was dropped on a scratched CFRTP surface. The scratches caused the liquid to bead-up as opposed to allowing the liquid to spread out and wet the surface, which would contribute to inaccuracies in this measurement. Along with this, contact angle measurements become more difficult to perform on slanted or upside-down surfaces, which could be necessary types of measurements for studying large parts used in the manufacture or repair of automobile or aircraft.

Figure 1.2: Image of water beading up on scratched surface of a CFRTP.

Finally, both contact angle measurements and CFRTP composite materials are susceptible to moisture and changes in relative humidity in ambient conditions [15, 21]. If contact angle is to be used in manufacturing-relevant environments, it needs to be able to accurately assess the

surface activation state in a variety of potential conditions and climates. Changes in relative humidity between environments may impact contact angle measurements, however, which could make it difficult to discern adequately-treated CFRTP materials from ill-prepared or un-activated materials. The CFRTPs themselves are also susceptible to the effects of moisture, as water content and saturation impact the underlying mechanical properties of the composite [15]. The act of dropping water (or other liquid) on the surface to perform contact angle measurements may therefore inadvertently and negatively impact the properties of the composite material if the liquid were to penetrate into the laminate material.

Due to the shortcomings of the quality control methods discussed above, a need exists for a quality control instrument or method that can non-destructively assess the surface activation state of plasma-treated CFRTP composite materials before bonding in environments of relevance to manufacturing. A new quality control method for assessing surface-activated composites should do four things: (1) be non-destructive to the material and the activation state of the surface, (2) be able to predict the bond strength of a material before the bonding procedure is performed, (3) be able to assess a wide variety of surface shapes and sizes, and (4) work in a variety of environmental conditions.

1.4 Motivating Work

There is a clear need for a non-destructive, quality-control instrument that can assess the surface activation state of plasma-treated CFRTP and composite materials in environments that are relevant to manufacturing. Previous research in our lab utilizing KPFM uncovered an interesting phenomenon that motivated this thesis work [12]. Summarized results of the study are shown in Figure 1.3 below.

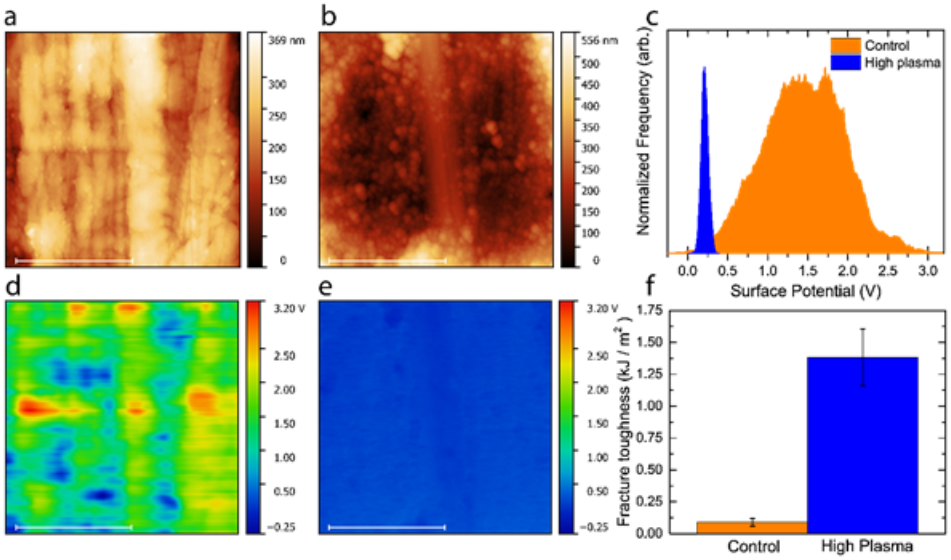

Figure 1.3: Topographic and surface potential maps of a control CFRTP coupon (a, d respectively) compared with maps of a plasma-treated coupon (b,e) measured by KPFM. The narrowing of the surface potential distribution of the plasma-treated samples compared to control (c) was then correlated with fracture toughness of the resulting bonded assembly (f) [12].

Surface potential distributions were measured across the surfaces of control (not-activated) and plasma-treated (activated) CFRTP coupons using KPFM. The results indicated an important phenomenon: plasma-treatment of a CFRTP coupon created a uniformly-activated surface as indicated by a narrow standard deviation of the surface potential across the sample surface compared to control coupons. The average surface potential value also decreased for plasma-treated CFRTPs when compared with control samples. These results were then correlated with fracture toughness of bonded assemblies made from nominally-identical plasma-treated and control CFRTP samples. A major conclusion of this study was that plasma-treatment of CFRTP surfaces creates a narrow surface potential distribution (i.e. a small standard deviation of surface potential) across the sample surface, which can be a predictor of the resulting bond strength of assemblies made from these materials. A positive correlation was developed between the inverse standard deviation of the surface potential, or $1/\sigma_{SP}$, and the fracture toughness of bonded assemblies, where large $1/\sigma_{SP}$ values typically measured on plasma-treated CFRTP surfaces predicted strong adhesive bonds while small $1/\sigma_{SP}$ values typically measured on control samples predicted weak bonds.

However, as mentioned above, current KPFM technologies are not suitable for manufacturing environments due to the high sensitivity of these measurements and their susceptibility to vibrational, environmental, and/or electromagnetic interference [1, 3, 9]. These devices are widely used in controlled laboratory settings, however the devices currently on the market are not developed with manufacturing or assembly lines in mind. This thesis work, therefore, aimed to take advantage of the novel discovery made above with KPFM measurements to develop a new instrument capable of robustly measuring the standard deviation of the surface potential across a sample surface in environments relevant to industries such as aerospace. A multi-probe Kelvin scanning (MPKS) instrument, which maintained the non-contact, non-destructive aspects of KPFM, was proposed and developed in this thesis work as a ruggedized tool for measuring standard deviations of surface potentials across CFRTP surfaces to assess the activation state of plasma-treated composites and predict the bond strength of resulting assemblies.

Chapter 2

Measurement Theory and Device Development

KPFM is a well-established measurement technique that takes advantage of differences in the work function of dissimilar materials to make relative measurements of surface potential values. By taking advantage of KPFM techniques and modifying the "off-null" method developed by Baikie [1, 2, 3] to make surface potential measurements, a general theory and set of governing equations was established that describe the Kelvin scanner prototype device operation.

2.1 KPFM Theory

Kelvin probe theory is based off of differences in material work functions between samples. The work function of a material is generally regarded as the energy required to excite an electron from the outer valence shell of an atom to the vacuum level. This material property varies between compounds due to differences in electronegativity, crystallinity, and composition, for example. Slight differences in these properties, even when dealing with the same compound or material, can result in discernable differences in the work function of the sample being measured.

When two conducting materials with dissimilar work functions are brought close together and connected in a circuit, charge flows between the materials. More specifically, electrons flow from the material with the lower work function to the material with the higher work

function to equalize the fermi energies of the materials. The flow of electrons induces equal and opposite charges on the material surfaces, establishing an electrical potential difference between the two materials. This potential difference is termed the contact potential difference (V_{CPD}) or surface potential (SP), and it is equal to the difference in the two materials' work functions before contact. In order to nullify the charge that builds up on the material surfaces when they are electrically connected, a backing potential (V_b) must be applied to the circuit such that, when $V_b = V_{CPD}$, the surface charges disappear and the materials return to their initial state. Thus, by scanning through V_b values in a given circuit, one can find the V_{CPD} between two dissimilar conducting samples by determining the V_b that nullifies the charge in the circuit. Once the V_{CPD} between the samples is known, as long as the work function of one of the materials is well-defined, the work function of the other material can be determined. This relative measurement can therefore be used to determine the work function of a material.

To make measurements of material work functions using KPFM, a conducting probe is brought into close proximity to a conducting sample surface, as seen in the basic diagram below (Figure 2.1, where the probe is positioned above a flat sample). The probe is usually much smaller than the surface area of the sample, varying from 10s of millimeters to microns depending on the resolution desired. The probe does not directly contact the sample surface, however the probe and sample are electrically connected (through an external power supply that provides the backing voltage V_b, as labeled in Figure 2.1) meaning that equal and opposite charges are induced on the sample and probe surfaces due to their differences in work functions. This means that a contact potential difference has been established between the two materials. The configuration of the probe and sample is that of a parallel-plate capacitor, where air acts as a dielectric between the two material surfaces.

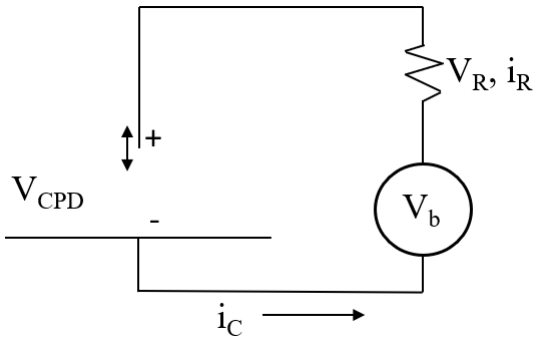

Figure 2.1: Basic diagram of measurement apparatus demonstrating probe (above) oscillating with respect to a stationary sample (below) and generating a current i_C that flows through the circuit.

One form of KPFM is performed by detecting oscillations induced in the probe as a result of electrostatic interactions between the probe and material surface and applying a backing voltage to the probe until its oscillation is nulled. When the probe stops oscillating, this means that the the charges on the probe and material surfaces have been nullified, indicating that V_b equals V_{CPD} or SP.

A different form of KPFM was utilized for the operation of this prototype, however. The Kelvin scanner prototype operates by oscillating the probe with respect to the stationary sample, similar to a vibrating parallel-plate capacitor. The continuous change in probe-to-sample distance changes the capacitance between the probe and the sample, which induces current flow through the measurement circuit. To determine the SP, the charge must be nullified in the circuit. This is done by sampling the waveform of the induced current in the circuit and determining what V_b value must be applied to the circuit to nullify or minimize the signal waveform. This is traditionally practiced by continuously amplifying and acquiring signals (in the form of current or voltage waveforms) as the probe oscillates with respect to the stationary sample and applying different V_b values until the null voltage is found. The V_b value that nulls the induced current in the circuit to 0 is the V_{CPD} or SP between the two materials. The following section develops the equations that govern the device operation (as discussed above) and shed light on the variables that most-significantly impact the ability of a probe to detect a signal from the sample.

2.2 Development of Governing Equations

As discussed above, the relationship between the probe and the sample can be treated as a capacitor with a dielectric (air) in between the two conductors. Capacitance is defined as

$$C := \frac{q}{V} \tag{2.1}$$

where C is the capacitance [Farads], q is charge [coulomb], and V is voltage [Volts] between the conductors. Rearranging this equation and differentiating with respect to time results in

$$V\frac{dC}{dt} + C\frac{dV}{dt} = \frac{dq}{dt} \tag{2.2}$$

where

$$\frac{dq}{dt} = i \tag{2.3}$$

or the the change in charge with time dq/dt [A] equals the current i [A] flowing through the circuit. As discussed in the previous section, the voltage between the conductors, or V_{CPD}, is a constant value equal to the difference between the work functions of the two materials

$$V = V_{CPD} = \frac{-(\phi_{probe} - \phi_{sample})}{e} \tag{2.4}$$

where ϕ_{probe} and ϕ_{sample} are the work functions [eV] of the probe and sample, respectively, and e is the elementary charge of an electron [e]. Since these values are constant with respect to time, the dV/dt term in equation 2.2 goes to zero. Combining this result with equation 2.3 leads to the following equation:

$$V\frac{dC}{dt} = \frac{dq}{dt} = i \tag{2.5}$$

The governing equation for a parallel plate capacitor may now be applied to the simplified equation above. The equation for a parallel plate capacitor is

$$C = \frac{A\epsilon}{z(t)} \tag{2.6}$$

where ϵ is the permittivity [F/m] of the medium between the two conductors, A is the probe tip area [m^2], and $z(t)$ is the distance between the probe and the sample [m]. Differentiating

this equation with respect to time and substituting it into equation 2.5 above results in the following relationship:

$$\frac{-V_{CPD}A\epsilon}{z^2}\frac{dz}{dt} = \frac{dq}{dt} = i \tag{2.7}$$

Based on equation 2.7, two criteria must be satisfied in order for current to flow through the measurement circuit. First, the probe and the sample must have different work functions, otherwise V goes to 0 as shown in equation 2.4 above. Second, there must be a change in distance between the probe and sample with time. In order to ensure these criteria are satisfied, dissimilar materials should be used for the probe and sample and one of the two materials must be oscillated with respect to the other.

When the probe and sample are electrically connected, equal and opposite charges are induced on their surfaces due to differences in their work functions, establishing a V_{CPD} between the materials (as seen in Figure 2.1 above). When the probe is oscillated with respect to the stationary sample while keeping the two surfaces parallel, current flow is induced in the circuit (i_c). Applying Kirchoff's current law that states that charge is conserved in a circuit, we know that the current induced by the probe oscillation must equal the current flowing through the resistor (i_R, seen in Figure 2.1). In other words,

$$V_{CPD}\frac{dC}{dt} = \frac{V_R}{R} \tag{2.8}$$

where V_R is the voltage [V] measured across the resistor and R is the resistance [Ohms]. Following this, Kirchoff's voltage law is applied stating that the sum of all potential differences across the components in a loop must be equal to 0. This means that

$$V_R = V_{CPD} - V_b \tag{2.9}$$

where V_b is the backing voltage [V] or DC bias applied to the circuit. Solving equation 2.8 for V_R and setting equal to equation 2.9 results in the following equation:

$$V_{CPD} - V_b = RV_{CPD}\frac{dC}{dt} \tag{2.10}$$

This can be further solved and simplified to

$$\frac{dC}{dt} = \frac{1}{R}(1 - \frac{V_b}{V_{CPD}}) \tag{2.11}$$

Combining equation 2.11 with equation 2.7 results in a general governing equation that describes device operation.

$$\frac{dC}{dt} = \frac{-A\epsilon}{z^2}\frac{dz}{dt} = \frac{1}{R}(1 - \frac{V_b}{V_{CPD}}) \tag{2.12}$$

The above equation, keeping in mind equation 2.5, illuminates several important characteristics about the measurment circuit of the device. First, the induced current is maximized at: (1) small inititial tip-to-sample distances z, (2) large probe oscillation amplitudes dz/dt, and (3) large probe tip areas A. Second, there is no induced current when the probe and sample are stationary with respect to each other. Finally, and most importantly, when $V_b = V_{CPD}$, the current goes to zero and the charge in the circuit is nulled. This is the key operating principle upon which this device was based. The following sections discuss how this principle was applied to assess surface activation states of materials.

2.3 Device Concept and Design

2.3.1 Basic Outline

Although laboratory-grade KPFM devices already exist for high-quality work function measurements in controlled environments, the device developed here aims to be ruggedized for manufacturing environments and was therefore built from scratch to better meet the quality control needs of the aerospace, automotive, and biomedical industries. The general diagram below (Figure 2.2) shows how key components of the device work together.

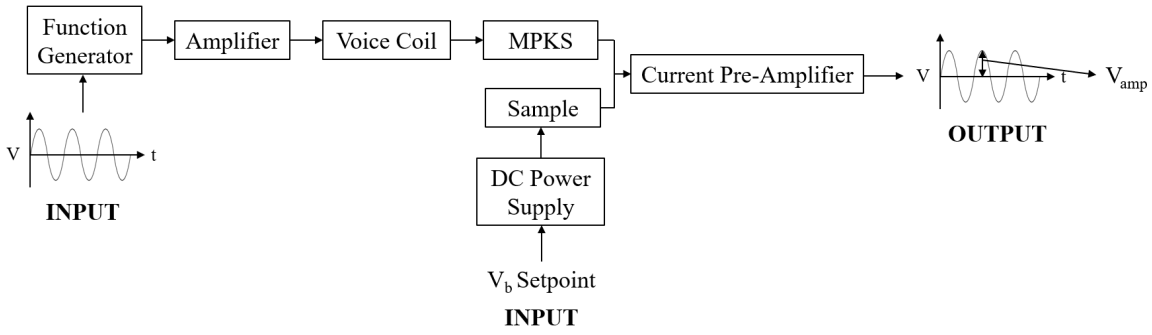

Figure 2.2: Basic measuremt diagram with key components labeled.

An oscillation frequency and amplitude are input by the user through the function generator. This input signal is sent from the function generator to an amplifier that amplifies the signal to the voice coil. The signal from the function generator governs the oscillatory motion of the voice coil, which in turn governs the oscillatory motion of the probe(s) with respect to the stationary sample. The current pre-amplifier amplifies the current induced in the circuit from probe oscillation, which is on the order of 10s-100s of picoamps, to a signal that is detected by a data acquisition device. The signal detected by the data acquisition device is a voltage signal, which is directly proportional to the current amplified by the pre-amplifier. The DC power supply provides the backing voltage to the circuit. By applying different V_b values to the circuit and measuring changes in the amplitude of the output signal (V_{amp}) from the current pre-amplifier, the voltage that nulls the output signal to zero can be determined, which corresponds to V_{CPD} or SP.

2.3.2 Device Design

The Kelvin scanner prototype can be seen in Figure 2.3 below with key pieces of equipment labeled. An important thing to note is that, because the currents being detected are on the order of 10s-100s of picoamps, the measurement circuit is highly susceptible to interference. Several shielding techniques were therefore implemented to improve the signal-to-noise ratio and isolate the measurement circuit from noise. First, the tip was located 10-12 inches away from the voice coil to reduce electromagnetic interference with the probe measurement, since the alternating magnetic field that induces oscillatory motion in the voice coil can couple

with the conducting probe(s) and induce noisy current flow in the circuit. Secondly, because most of the device frame is made from aluminum, the frame acts as an antenna for noise induced by electromagnetic interference produced by the surrounding equipment. Therefore, most metal components of the frame, along with parts of the micrometer-positioning stage, were grounded. Along with this, rubber mats were placed underneath the device frame and sample stage to isolate errant vibrations caused by the voice coil. This helped keep the device frame stable and ensured that the sample was stationary with respect to the oscillating probe. Finally, all wires in the measurement circuit were shielded to further reduce noise in the measurement.

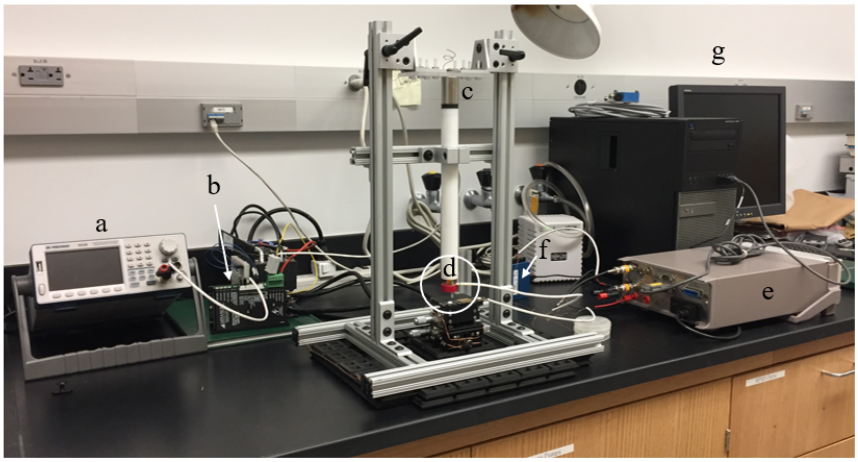

a. Function Generator
b. Signal Amplifier
c. Voice Coil
d. Probe
e. Keithley Picoammeter/ Voltage Source
a. DAQ Board
b. Computer Controller

Figure 2.3: Image of the device developed in lab with key components labeled.

The equipment labeled in Figure 2.3 operates as described above. The Keithley 6482 Picoammeter serves as both the DC power supply that applies V_b and the current preamplifier, as it has both capabilities built into its hardware. The data acquisition (DAQ) device acquires the amplified analog signal output by the Keithley device and transfers the data to the computer for analysis. A diagram detailing this measurement circuit can be seen in Figure 2.4 below. The USB-6000 Analog Input Recorder (labeled below) is the DAQ device that acquires the signal and transfers it to the computer monitor. The sample stage has 3-axis (x, y, and z) motion capabilities with 10-micrometer positioning control. The stage is grounded to reduce interference with the measurement. An insulating material is placed between the stage and the sample to ensure that the sample is not grounded.

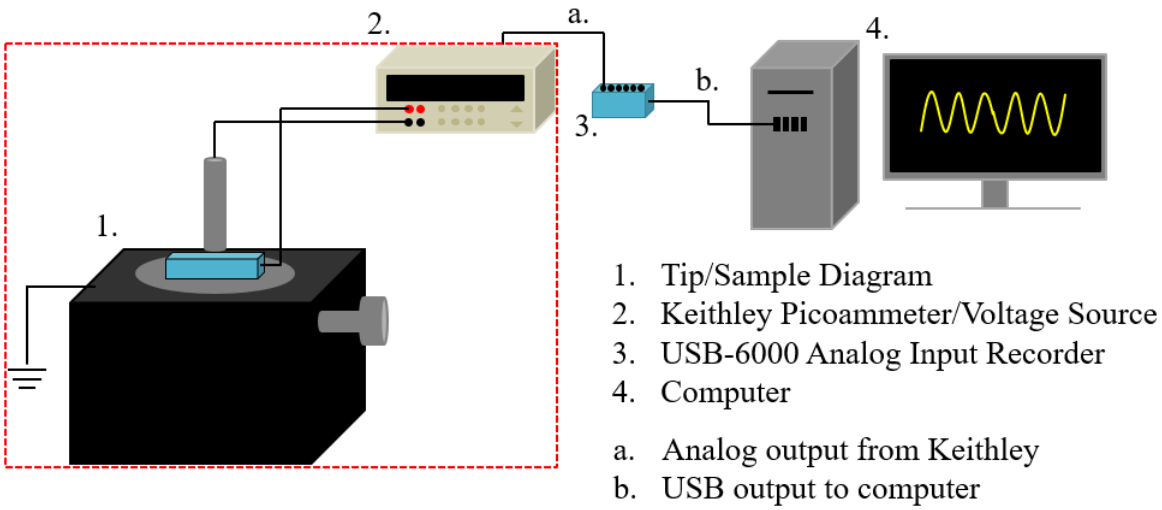

Figure 2.4: Diagram of measurement circuit (emphasized by the red box) and signal acquisition.

To acquire the signal for processing, a LabVIEW program was developed to communicate with the USB-6000. By manually programming a sweep of V_b in the Keithley and synchronizing the sweep with the LabVIEW acquisition program, a signal could be acquired at each V_b applied to the circuit. After a sweep was completed, the LabVIEW program exported the acquired data to an Excel document. A MATLAB program was developed to import this data, process it, and ultimately calculate the SP value for that measurement. A Python script was recently developed such that all of these functions (the V_b sweep, data acquisition, and data analysis) could be executed in a single environment, outside of LabVIEW and MATLAB, thus eliminating the need to purchase these expensive software packages and improving efficiency of measurement. The following section describes the SP measurement process and data analysis steps in more detail.

2.4 Measurement and Data Analysis

2.4.1 Measurement Process

This section aims to describe more specifically how the instrument measures the SP and standard deviation of that SP across a sample surface. To make an accurate measurement, the probe has to be brought in close proximity to the sample surface. Although the required tip-to-sample distance may vary as the probe area or oscillation amplitude increases, generally the probe needs to be within a few hundred microns of the sample to detect a signal. This proximity can be visualized in Figure 2.5 below, where a single probe with a 3-mm diameter tip was used to make measurements of a CFRTP surface.

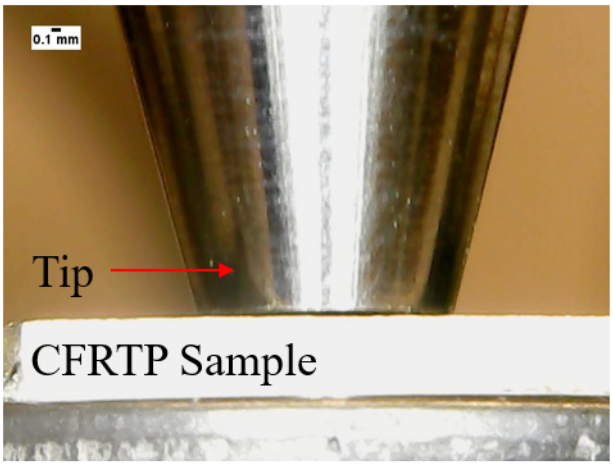

Figure 2.5: Image of probe proximity to sample surface when making measurements in the single-probe configuration.

Once the probe is in close proximity to the sample surface and a signal can be detected when the probe is oscillating, the V_b sweep must be programmed. This is done by manually entering the V_b values into the Keithley in the desired order for voltage sweeping. A randomized order of V_b values was initially established and kept constant for every sample measurement made with this device. The V_b values ranged from -0.5 to 1.5 Volts in 0.1 Volt increments, resulting in 21 different voltages that were scanned for every measurement. This scan of 21 V_b values was performed three times at a given site on the sample surface to allow for data averaging

later on in the analysis that reduced the effect that noise had on the measurement. The total data acquisition process therefore acquires 61 signals (three sets of signals at 21 different V_b values), taking just over one minute to acquire and store the data.

2.4.2 Data Analysis and Determining SP

The data analysis steps were performed in MATLAB. A script was written to import the signal data acquired by the DAQ device and calculate the SP of the sample. A modified version of the off-null technique developed by Baikie [1, 2, 3] was used to calculate the SP through several steps. First, the current detected by the Keithley was converted into a voltage signal, acquired by the DAQ device, and imported into MATLAB. Next, the Fourier transform of the signal was taken to isolate the effect the probe oscillation had on the signal from noise in the circuit. Finally, a plot of signal amplitude versus backing voltage was developed, where the intersection of two linear fits on the data determined the SP value of the measurement.

Because of the high sensitivity of the circuit to electromagnetic interference and other sources of noise, signal processing must first be performed on the acquired signal. Assuming the sample is stationary and the probe is oscillating at a known frequency, changes in the voltage waveform output by the Keithley can be traced back to the frequency of oscillation of the probe. Therefore, taking the Fourier transform of the output waveform and looking at V_{amp} as a function of frequency can distinguish signal amplitude changes caused by noise from changes caused by the tip oscillation. Example MATLAB plots of these steps are visualized below in Figure 2.6. The signal detected at 60 and 120 Hz are the result of the line, or utility, frequency used here in the United States. The signal detected at 110 Hz is a result of the oscillation frequency of the probe, which was set to 110 Hz using the function generator.

For clarification, although the Keithley outputs a voltage waveform that is acquired by the DAQ device, it is actually directly measuring changes in current in the circuit (as discussed previously). Since current and voltage are proportional, however, the current waveform detected by the Keithley is directly proportional to the voltage waveform it outputs to the DAQ device. In the following plots, the "Signal Voltage" and "Signal Amplitude" (seen on

the y-axis of the plots) refer to the voltage signal output by the Keithley and acquired by the DAQ device.

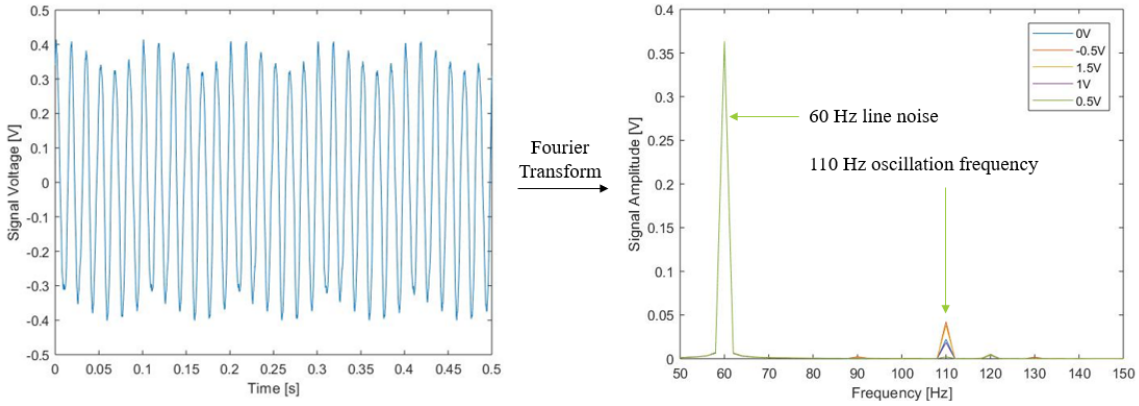

Figure 2.6: MATLAB plots showing an example of an acquired signal waveform and the combined Fourier transform plot of five different signals (each corresponding to a different V_b).

Each line in the Fourier-transformed plot is a signal at a different V_b value (0, -0.5, 0.5, 1, and 1.5 Volts). Isolating the signal amplitudes at the 110 Hz probe oscillation frequency shows that the signal amplitude clearly changes as a function of V_b, as demonstrated in Figure 2.7 below. The low resolution of the Fourier transform plot is a direct function of the measurement duration. Since resolution in the frequency domain is inversely related to the sampling duration in the time domain, resolution in the Fourier plot is lost as sample time is decreased. Signals were acquired for 0.5 seconds in order to reduce measurement time, thus limiting the resolution in the frequency domain to 2 Hz.

Plotting the signal amplitude as a function of backing voltage, or V_{amp} as a function of V_b, results in the plot seen below in Figure 2.8. As mentioned above, 21 V_b values from -0.5 to 1.5 V were used and signals were sample sampled three times at each V_b value to reduce noise. The V_{amp} values plotted are averages of the three measurements made at each V_b along with standard deviation bars across those three measurements.

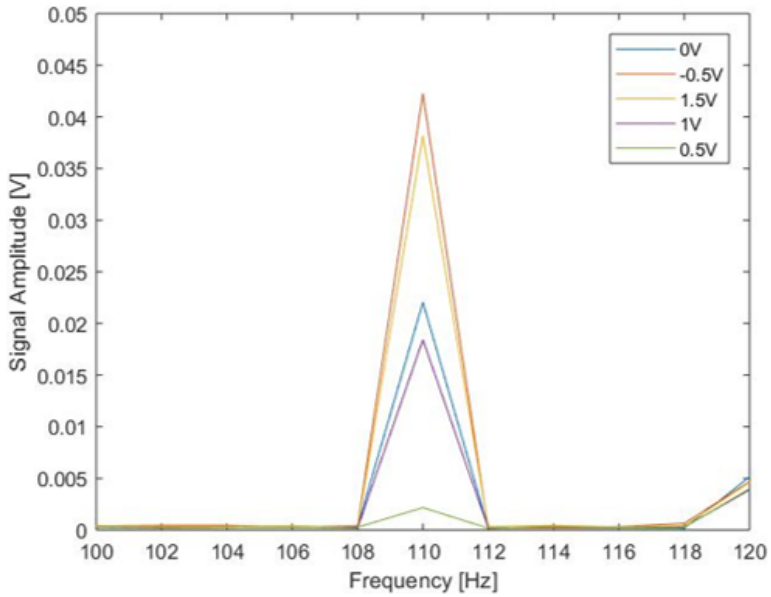

Figure 2.7: MATLAB plot focusing in on 110 Hz frequency of Fourier-transformed signal.

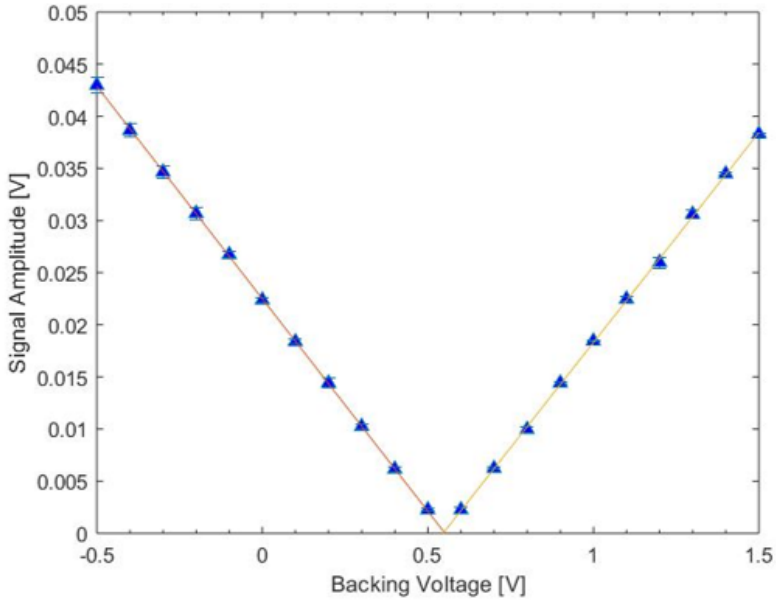

Figure 2.8: Example MATLAB plot of signal amplitude V_{amp} vs V_b after extracting points from the 110 Hz frequency of the Fourier-transformed signal.

To determine the SP of the sample, the V_b value that nulls the signal to zero needs to be determined because V_b = SP at that point. The signal is nulled when its amplitude, or V_{amp}, is minimized or equal to the background V_{amp} value in the circuit. This null point can be determined by performing two separate linear fits, one to each side of the v-shaped curve seen in Figure 2.8, and finding the intersection of these lines with each other. One could also find where the linear fits each equaled the background V_{amp} value and then averaged these values together, however this value was found to be equal to the value calculated by determining the intersection of the lines within one standard deviation. When performing these linear fits, the two V_b values closest to the null voltage (i.e. the two V_b values corresponding to the two smallest V_{amp} values) were excluded from the fit due to a general increase in noise when approaching the null voltage [3].

The calculated intersection of the two linear fits, excluding the two points nearest to the null voltage, is the SP at the site being probed. Since the diameter of the probe tip used (on the order of 3 mm or 5 mm) is much smaller than the dimensions of the samples being measured (usually 10 x 10 mm up to 2" x 1"), to get an SP map of a sample surface multiple sites need to be measured across the surface. Once an SP map of the surface is made, an average SP value can be calculated for the surface and a standard deviation of that value across the surface can be determined.

This measurement principle allows for the SP mapping of a material surface and the calculation of the standard deviaiton of that SP across the surface through the measurement of multiple sites on the sample. Applying these principles to the Kelvin scanner device proposed in this work allows for the instrument to measure standard deviations of SPs across a sample surface, which is a fundamental measurement for distinguishing between plasma-treated and control CFRTP materials, as discussed in Chapter 1. Since the motivation behind this work revolves around the novel discovery that plasma-treatment of CFRTP materials creates a narrow standard deviation of SP across the sample surface compared to control samples, implementing the measurement principles discussed here will allow for the reproduction of the previous KPFM results by the new Kelvin scanner instrument to determine if the new instrument can distinguish between plasma-treated and control CFRTP samples and therefore be relevant for quality control purposes in manufacturing environments. Correlations of the standard deviation of SP values measured by the Kelvin scanner prototype with fracture toughness of bonded assemblies can further demonstrate the instrument developed in this

thesis work can accurately predict the bond strength of the resulting CFRTP assemblies. The testing discussed in the following chapters details the SP and standard deviation measurements made with single- and multi-probe heads and how these measurements correlate with CFRTP assembly bond strength.

Chapter 3

Single-Probe Prototype Testing

This chapter details the testing of the single-probe Kelvin scanner prototype on CFRTP materials to see if it could distinguish between control and plasma-treated samples. Materials and methods for preparing the CFRTP samples for testing are presented along with the results from measuring the samples with the developed instrument and discussion of the implication of the results.

3.1 Sample Preparation Methods

3.1.1 Preparing CFRTP Coupons

The CFRTP coupons prepared for these experiments were composed of unidirectional carbon fibers set in a polyether-ketone-ketone (PEKK) matrix. The coupons were received in 3" x 6" sheets that were then cut into 10mm x 10mm squares to be used for the experiments. The samples were approximately 0.8 mm in thickness.

Since CFRTP materials are notoriously susceptible to water saturation and temperature, the samples all went through the same pre-treatment processing steps to establish a baseline across the sample set. The coupons first went through a cleaning procedure involving consecutive sonicated solvent baths in acetone and isopropanol. After blowing the samples dry with compressed air, the coupons were then placed in a furnace for three days at 80-90 ^{o}C to dry the samples and drive out any excess moisture. After drying, the samples were then placed in incubators at a controlled relative humidity (43-45%) to establish the same level

of water saturation across the CFRTP coupon set. The samples remained in the incubator for a minimum or 24 hours before being removed for plasma-treated or measurement. After treatment or between measurements, the samples generally were stored in ambient lab conditions, although there were several experiments performed where the samples were stored back in the relative humidity chambers between measurements.

Although the carbon fibers embedded in the thermoplastic matrix were inherently electrically conductive, the carbon fibers were not fully accessible from the external surfaces of the samples. To ensure that the CFRTP coupons would be in electrical contact with the measurement circuit, the bottom and the two sides of the sample perpendicular to the direction of the carbon fibers were coated in silver conducting paint and the sample was subsequently mounted on a stainless-steel disc. This step was performed before any plasma-treatments or measurements were performed in order to preserve the activation state of the sample surface. Figure 3.1 below displays the CFRTP samples used in these tests and what samples looked like when attached to the stainless-steel disc. The vertical alignment of the carbon-fibers can also be seen in the figure.

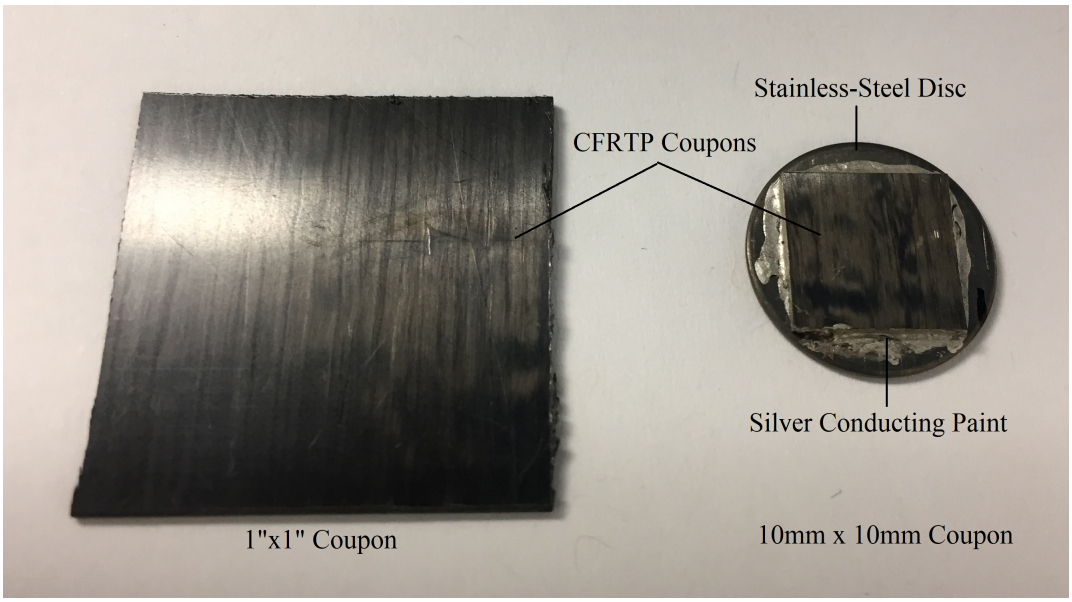

Figure 3.1: CFRTP samples used for testing, including an example of a coupon mounted on a stainless-steel disc.

3.1.2 Plasma-Treatment of Coupons

The surface-activation technique used for treating the CFRTP samples consisted of a low-temperature plasma treatment. The plasma consisted of a mixture of nitrogen (N_2), argon (Ar), and oxygen (O_2). The plasma-treatment system was a home-built setup that can be seen in Figure 3.2 below. The laptop computer allowed for remote control of the mass flow controllers to set the inlet gas flow rates. The rough pump kept the reactor under vacuum during and after treatment. The electrodes generated the plasma up stream of the treatment chamber so that the plasma would flow downwards and interact with the sample surface. The plasma was controlled by an external RF power supply and matching network that allowed for adjustment of the plasma power. The treatment chamber had viewports on three sides to allow for proper alignment of the sample with respect to the plasma. The fourth side of the treatment chamber had an arm that allowed for the insertion of the sample into the treatment chamber.

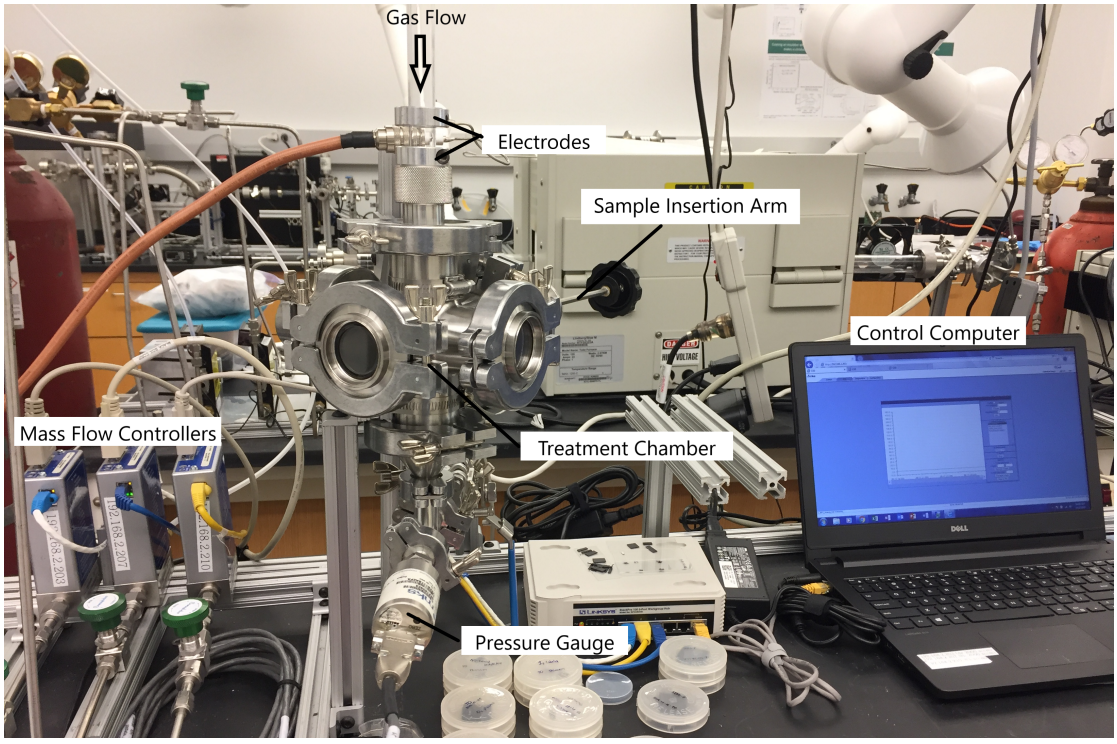

Figure 3.2: Image of the plasma reactor used for sample treatment with important components labeled.

The basic treatment procedure was as follows. After securing the CFRTP coupon to the stainless-steel disc with conducting paste and allowing the paste to dry, the sample was attached to the ledge on the end of the insertion arm using carbon tape (seen below in Figure 3.3). This would keep the sample in place so that the gas flow inside the chamber did not blow the sample off the stage during treatment. The sample was then inserted into the chamber and sealed off from ambient. After lining up the sample so that it was parallel to and centered on the opening of the plasma reactor tube, the valve to the rough pump was opened and the treatment chamber began pumping down. After pumping down for two minutes, usually to a base pressure of 0.06-0.13 mTorr, the valves to the inlet gas lines were opened and the inlet gas flow rates were set on the laptop. The setpoints for the gas flows were 175 sccm Ar, 27 sccm O_2, and 55 sccm N_2 for all experiments. Fluctuations in the pressure gauge from experiment-to-experiment and day-to-day reported the chamber pressure as being anywhere from 0.6-0.9 mTorr. Due to these fluctuations, the gas flow rates and the ratios of these flows to each other were chosen as the parameters to control and keep constant from experiment-to-experiment.

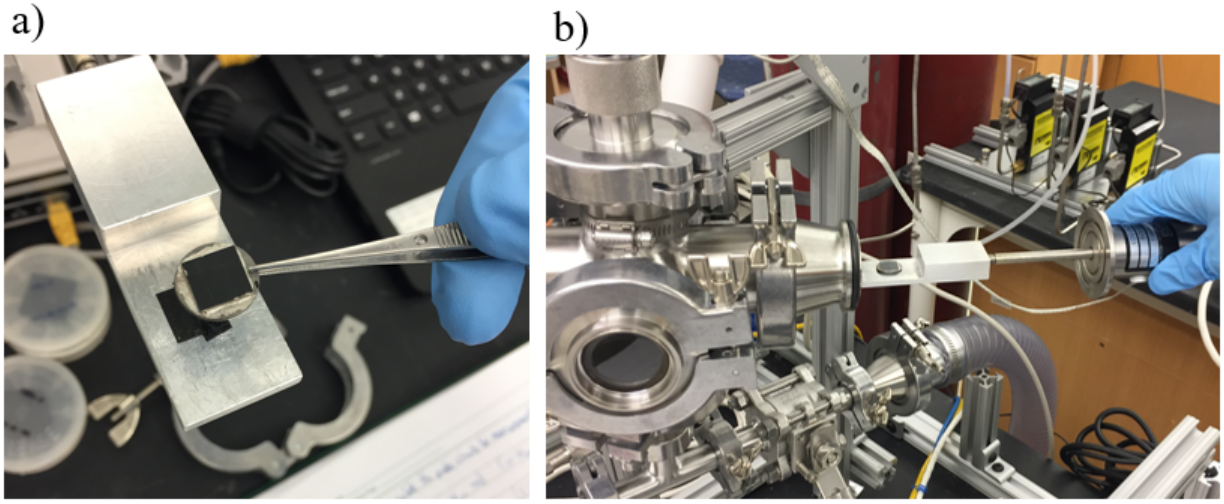

Figure 3.3: Attaching a sample to the insertion arm (a) and inserting the sample into reactor for plasma treatment (b).

After allowing the gas flows and resulting pressure to stabilize, usually on the order of 10s of seconds, the plasma was lit using the RF power supply and matching network. The plasma power was set to 50 Watts for all treatments. Treatments lasted for 4 minutes, after which

the plasma was shut off, the chamber was re-pressurized, and the sample was removed from the reactor. For each treatment, the treatment time, plasma power, gas inlet flow rates, and the reactor pressure were recorded. An image of the plasma treatment process is included below in Figure 3.4.

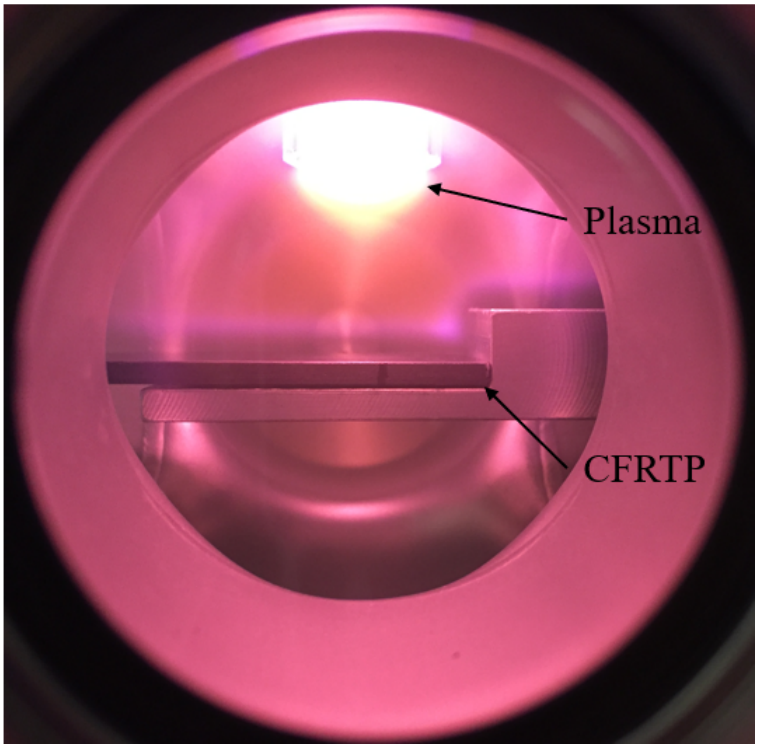

Figure 3.4: Plasma-treating 2" x 1" CFRTP sample.

3.2 Testing Single-Probe Device

3.2.1 Experimental Parameters

The experiments performed here aimed to test the prototype Kelvin scanning device to see if it could distinguish between plasma-treated and control CFRTP samples based on measurements of SP distributions. To do this, sets of plasma-treated and control samples were

prepared by the methods discussed above. Samples were stored in ambient lab conditions after plasma-treatment along with accompanying control samples.

A stainless-steel probe with a tip diameter of 3 mm was used to make SP measurements of the CFRTP surfaces. Stainless-steel was used as the probe material because of its machinability, relative inertness, and it's difference in work function relative to the expected work function of the CFRTP materials. When measuring CFRTP samples, the sample was brought in close proximity to the oscillating probe tip until the probe detected a change in the acquired voltage signal. The probe-to-sample distance needed to be on the order of several hundred microns to detect a signal change with the probe used for these measurements. This proximity can be seen in Figure 2.5 above.

The first experiment performed with the single-probe Kelvin scanner prototype was a blind test of three CFRTP coupons, two of which were plasma-treated by another student in lab. Measurements of these samples were made before handing over the samples to the student and in the three days after receiving them back from the student. To determine the SP map of the sample surface, four measurements were made on each sample, effectively dividing the sample into quadrants. One of the quadrants from Sample B had significant surface damage as a result of handling, so it was excluded from measurement. The average and standard deviation of the SP measurements was then determined across the sample surface based on the measured sites. The measurement sites were held constant (i.e. the same sites were measured each time) over the duration of the testing.

The other experiments performed with the single-probe Kelvin scanner prototype consisted of varying time scales of testing. The first timescale test involved the measurement of a CFRTP coupon before being plasma-treated and then in 30-minute intervals after plasma-treatment (including a measurement made immediately after treatment). The SP of the sample was determined by making nine measurements on the sample surface, effectively dividing the surface into a 3 x 3 grid. These sites were again held constant from measurement to measurement.

The second timescale experiment measured a single CFRTP coupon before plasma-treatment and then at random time intervals over the course of the five days succeeding treatment. SP maps of the sample surface were made by measuring four random sites across the sample surface for each measurement.

The final set of timescale experiments consisted of measuring a set of three CFRTP coupons before plasma-treatment and then every day after treatment for nine days. The SP of the sample was determined by measuring the same nine sites on the sample surface (similar to the short time-scale experiment) for each set of measurements on each sample. These experiments all aimed at testing the efficacy of the quality control instrument proposed and developed here to see if the Kelvin scanner prototype could a) distinguish between plasma-treated and control CFRTP samples and b) make this distinction over various time scales.

3.2.2 Results

The single-probe Kelvin scanner device was able to distinguish between plasma-treated and control (untreated) CFRTP composite samples by measuring changes in the standard deviation of SP across the sample surface. The standard deviation of SP decreased for plasma-treated samples compared to control samples or measurements made pre-treatment. These results were reproducible over the course of several hours and several days after plasma-treatment of the CFRTP materials.

The Kelvin scanner prototype detected a decrease in SP and narrowing of the standard deviation of that SP for two of the three samples (Samples A and C) measured in the blind test, as seen in Figure 3.5 below. The measured SP values for Samples A and C approached each other with time and had smaller standard deviations on their SP when compared to Sample B. The standard deviations of the SP values measured on the surfaces of Samples A and C also approached each other with time. Based on the narrowing of the standard deviation of SP for Samples A and C when compared with Sample B, it was predicted that those two coupons were plasma-treated while Sample B was left un-treated. The student who treated the samples confirmed that this prediction was correct.

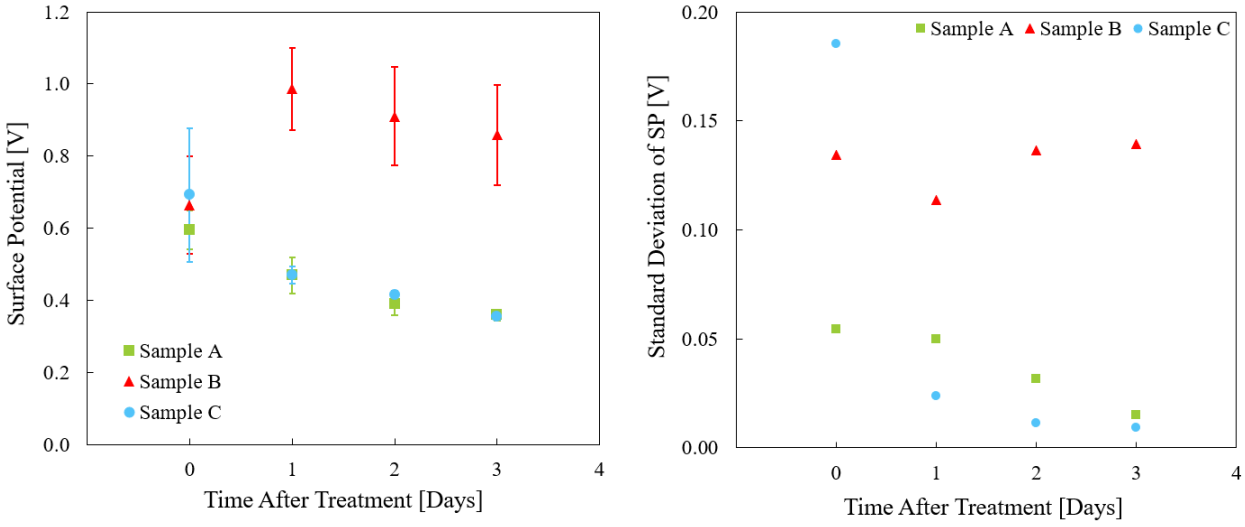

Figure 3.5: Results of the blind test performed by the single-probe Kelvin scanner prototype to distinguish between control and plasma-treated CFRTP samples.

The short timescale results indicated that the Kelvin scanner prototype could distinguish the narrowing of the standard deviation of SP in the immediate hours after plasma-treatment, as seen below in Figure 3.6. The pre-treatment measurement is plotted at time = 0 hours, and the subsequent measurements were all made at the specified time after treatment. The control, or pre-treatment, measurement had a large standard deviation of the measured SP of the sample, as can be seen in the plot on the right. This standard deviation decreased for subsequent measurements made after treatment. The SP value measured for the sample increased, also accompanied by a large standard deviation of this value, immediately after plasma-treatment, which is demonstrated by the second point on the left plot. Over the four hours after treatment, the standard deviation approached a constant value that was an order of magnitude less than the value calculated from the pre-treatment measurement.

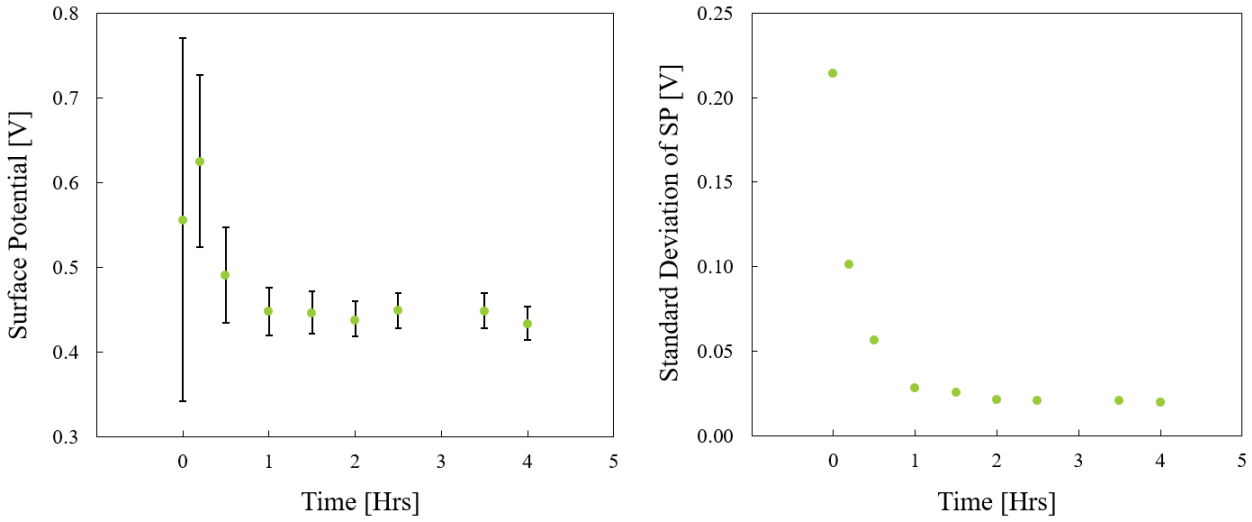

Figure 3.6: SP measurements (left) and the standard deviation of those values (right) measured by the single-probe Kelvin scanner prototype in the first five hours after treatment.

The results of the first long timescale experiment performed are displayed below in Figure 3.7 and Table 3.1. The results paralleled the short timescale experiment in that 1) the standard deviation of the measured SP was generally larger for the pre-treated (control) measurement than for post-treated measurements and 2) the measured SP increased with a large standard deviation of the measurements for the test performed immediately after plasma-treatment. The standard deviation of SP for the control sample was much smaller than previously measured values, demonstrating the non-uniformity of these CFRTP materials. However, the standard deviation of SP post-treatment was still generally smaller than the value calculated pre-treatment. The values plotted in Figure 3.7 below are tabulated in Table 3.1 as well, where σ_{SP} is the standard deviation of the measured surface potential across the sample surface.

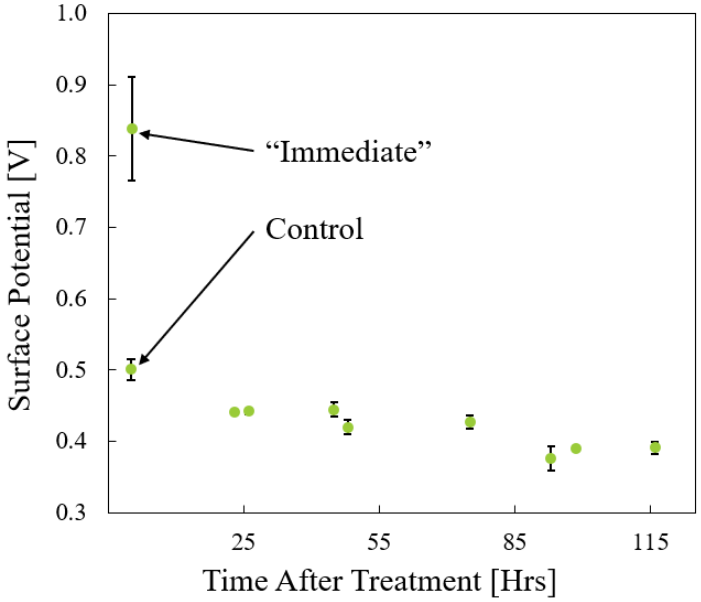

Figure 3.7: SP measurements made by the single-probe Kelvin scanner prototype on a single CFRTP sample in the first few days after treatment.

Table 3.1: Tabulated Results of First Long Timescale Experiment on Single CFRTP Sample

Time [Hrs]	**SP [V]**	σ_{SP} **[V]**
Before (Control)	0.5009	± 0.0149
Immediate	0.8381	± 0.0728
23	0.4418	± 0.0022
26	0.4423	± 0.0038
45	0.4444	± 0.0101
48	0.4199	± 0.0099
75	0.4266	± 0.0094
93	0.3761	± 0.0168
99	0.3906	± 0.0021
116	0.3914	± 0.0084

The final long timescale experiments, performed on three CFRTP samples, also paralleled the above results. As seen in Figure 3.8 and Table 3.2 below, the standard deviations of the SP values decreased for samples post-plasma-treatment. A spike in SP and standard deviation was again seen for the measurements performed immediately after plasma-treatment. Figure 3.8 shows the individual measurements performed on each sample, with the control or pre-treatment measurement plotted at t = 0 days. Table 3.2 aggregates the results from Figure 3.8, taking an average across all three samples for a given measurement.

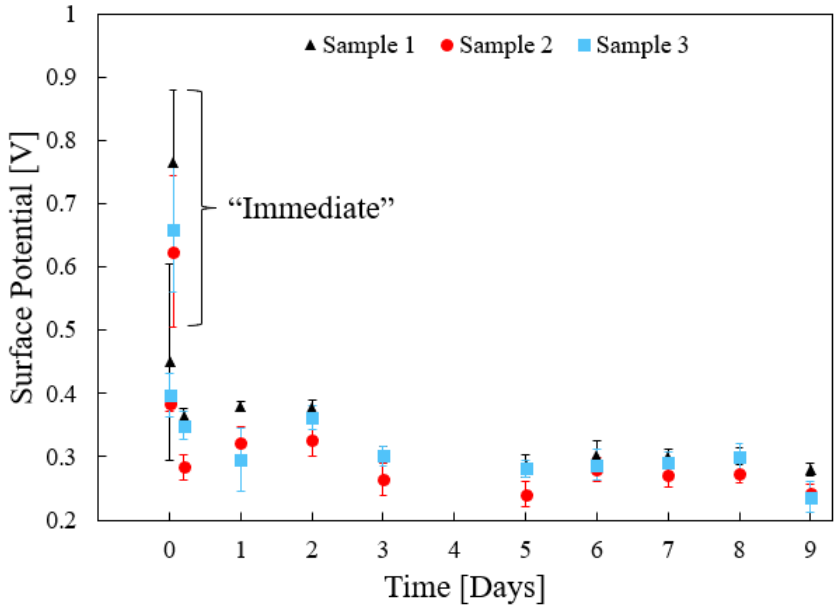

Figure 3.8: SP measurements and the standard deviation of those values measured by the single-probe Kelvin scanner prototype on a three CFRTP samples over a 9-day period.

Table 3.2: Averaged Results from Long Timescale Experiment on Multiple Samples

Time	**Average SP [V]**	**Average σ_{SP} [V]**
Before (Control)	0.4109	± 0.0681
Immediate	0.6831	± 0.1114
5 Hrs	0.3322	± 0.0183
1 Day	0.3325	± 0.0284
2 Days	0.3557	± 0.0186
3 Days	0.2894	± 0.0183
5 Days	0.2694	± 0.0166
6 Days	0.2896	± 0.0227
7 Days	0.2873	± 0.0162
8 Days	0.2912	± 0.0172
9 Days	0.2609	± 0.0124

3.2.3 Discussion and Conclusions

The results presented above demonstrate the promise of this prototype Kelvin scanner device to serve as a non-destructive quality control instrument for assessing the surface-activation state of plasma-treated CFRTP composite materials. In a blind test, the device could discern between unknown control and plasma-treated coupons based on changes in the measured SP values and the standard deviation of those values across a sample surface. This would allow a device operator in industry to make a basic go/no-go decision on whether a material had been adequately prepared by plasma-treatment.

Although direct comparison of the measured SP values could be used in certain situations to distinguish between plasma-treated and control CFRTP coupons, this should not be the metric used for comparison due to the impact that changes in ambient conditions (e.g. relative humidity, temperature) have on the measured SP values [9]. For this reason, the standard deviation of the measured SP values at a given time should be used as the metric for comparison instead. Therefore, by comparing the standard deviations of SP measurements made by the single-probe prototype across a sample surface on control samples and plasma-treated samples, one should be able clearly distinguish between the two materials.

The results from the timescale experiments proved the ability of the device to measure these changes in standard deviation and therefore make the distinction between control and plasma-treated samples. In the hours and days after plasma-treatment, the single-probe Kelvin scanner prototype routinely measured narrow standard deviations of SP across plasma-treated CFRTP surfaces when compared with control or pre-treated samples. This further demonstrates the value of this device in manufacturing environments where no sufficient non-destructive quality control methods exist for assessing surface activation of plasma-treated CFRTP materials.

The anomaly seen when making SP measurements with the prototype instrument immediately after plasma-treatment is believed to be a function of surface- or bulk-charging of the material during treatment. Since plasma-treatment involves reactive, ionized molecules continuously bombarding, etching, and/or reacting with a material surface, it is likely for charge to build up within the material if the material is not properly grounded. Although the arm used for inserting samples into the chamber is grounded, the sample itself is attached to the arm with carbon tape, which is only partially conducting. Any charge that builds up in/on the material during treatment, therefore, has difficulty trying to escape since the sample itself is not completely grounded during treatment. This is believed to be the reason why large SP values and standard deviations of those values are found when transporting the sample immediately from the treatment chamber to the single-probe prototype for measurement. Built-up charge is likely dissipating for the duration (and even in the time after) of the measurement made immediately after plasma-treatment. The stability of the SP and standard deviation measurements on plasma-treated samples in the hours and days after treatment indicates that the excess charge has had time to dissipate, leaving a chemically- and electrically-stable material and surface that is distinctly different from control samples. This trend will be discussed further in Chapter 5.

In conclusion, the single-probe prototype Kelvin scanner can accurately distinguish between control (untreated) and plasma-treated CFRTP materials by measuring and comparing the standard deviations of SP across the material surfaces. Plasma-treated samples had narrower distributions of SP, as indicated by a smaller standard deviation calculated across a sample surface, when compared with control samples. This result paralleled the results presented in Chapter 1 that motivated this project. However, since this project used a different Kelvin scanner device and different plasma-treatment system than what was used in the motivating

work, correlations of SP measurements made with this prototype with meaningful material properties were sought to understand if the measurements made with this instrument could prodict bond strength. For this reason, mechanical testing was performed on bonded CFRTP assemblies to develop a correlation between fracture toughness of control and plasma-treated CFRTP assemblies and the SP and standard deviation measurements discussed here. The following chapter discuss the methods and results of these mechanical tests.

Chapter 4

Mechanical Testing of Bonded CFRTP Assemblies

This chapter details the mechanical testing performed on bonded CFRTP assemblies to ensure that the measurements made with the single-probe Kelvin scanner prototype could be correlated with bond strength in the resulting materials. Because the results that motivated this project correlated narrow surface potential distributions with fracture toughness of bonded assemblies, the mechanical testing experiments performed here aimed to reproduce these results except with our own resources (plasma reactor and single-probe prototype discussed in the previous chapter) to establish the efficacy of the developed instrument. The following experiments aimed at correlating bond strength of expoxy-bonded CFRTP assemblies as determined by lap-shear testing with the SP and standard deviation results reported in Chapter 3.

4.1 Materials and Methods

4.1.1 CFRTP Coupon Preparation

The CFRTP coupons used in bonding went through the same preparation steps as discussed in Chapter 2. The coupons used for this testing were the same CFRTP materials discussed above except they were cut into larger (1" x 1") squares. Two sets of samples were prepared for bonding: one set of six control assemblies and one set of ten plasma-treated assemblies

(following the same treatment steps as previously discussed). The plasma-treated samples were treated at different durations out from bonding, since the activation states among these samples were similar across the set according to the surface potential maps and standard deviations shown in Chapter 3.

4.1.2 Bonding Procedure

Bonded assemblies of the CFRTP coupons were made by gluing two 1" x 1" coupons together using an epoxy resin. For control samples, the bonding was performed on two un-treated control CFRTP coupons. The plasma-treated assemblies consisted of two plasma-treated samples with their activated surfaces bonded together. The bond area, or sample-sample overlap, and the bond thickness were kept constant for all assemblies produced.

Sample-to-sample bonding was performed utilizing Loctite Hysol EA 9394 AERO Epoxy. This two-part epoxy was mixed together to initiate the curing process and then applied in a thin layer to half of the surface of two CFRTP samples such that the epoxy-coated area of each of the samples was 0.5 in^2. To control the bond thickness, a thin (0.15 mm) fabric scrim was cut into a 0.5" x 1" rectangle and placed on one of the epoxy-coated samples. The two samples were then pressed together such that their 0.5" x 1" epoxy-coated areas overlapped keeping the scrim between the two surfaces. It was also important to ensure that the carbon fibers of both samples were aligned (or parallel with each other) so that the mechanical strength of the individual samples would be preserved when experiencing the high loads associated with lap-shear testing. Pressing the assembly together squeezed out any excess epoxy and reduced the bond thickness such that it could be approximated as the thickness of the scrim for each assembly. The diagram shown below in Figure 4.1 demonstrates what this bonding procedure looked like in practice.

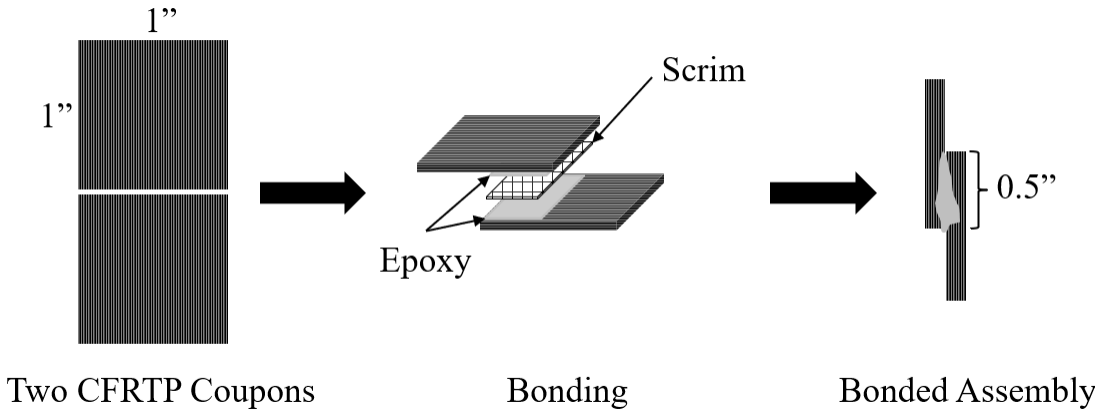

Figure 4.1: Diagram of bonding process for two CFRTP coupons.

Once the samples were hand-pressed together, they were then placed under bricks to keep a constant pressure of 5 psi applied to the assemblies. This ensured that the bond thickness would not expand during the curing process. The assemblies were then moved to a furnace, with the bricks still positioned atop the assemblies, and baked at 75 °C for three and a half hours. This baking process, although not necessary, accelerated the curing of the epoxy resin. After baking, the samples were removed from the furnace and kept in ambient lab conditions, still under the applied pressure of the bricks, for at least 24 hours prior to testing.

4.1.3 Universal Testing Machine Apparatus

The apparatus used for the lap-shear testing of the bonded assemblies was an Instron 5583 electro-mechanical Universal Testing Machine. The machine consisted of a set of wedge grips, one mounted to the frame and the other mounted to a moveable load, which were hand-tightened to hold the sample firmly in place. Different sized loads (500 N, 5 kN, or 150 kN) could also be applied to the materials being tested by switching out the load cells located above the wedge grips. The machine was programmed to pull the sample apart at a constant crosshead speed, continuously measuring and recording the applied load until failure occurred. Figure 4.2 below displays the important components of the Instron Universal Testing Machine used for lap-shear testing.

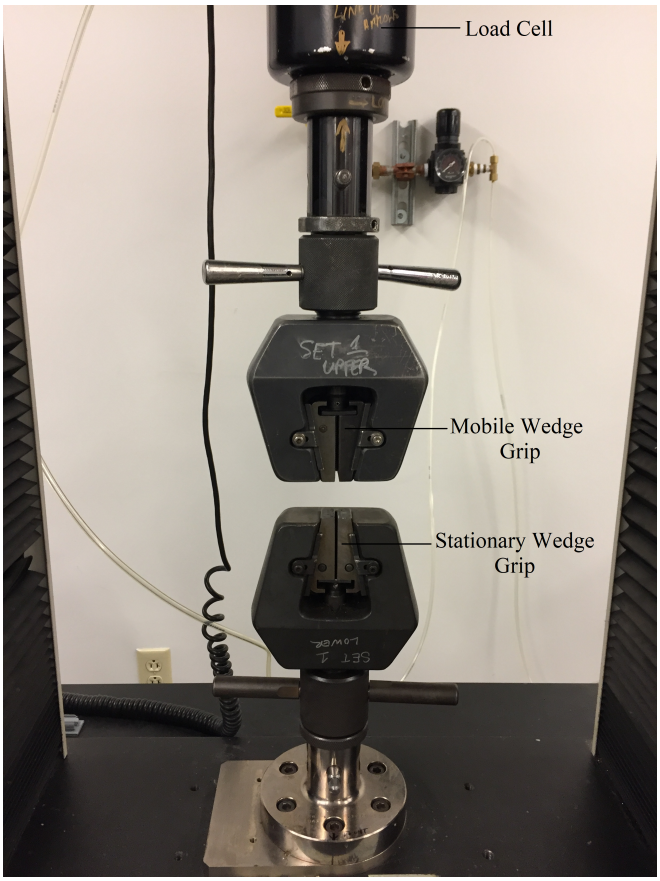

Figure 4.2: Important components of the Instron Universal Testing Device.

4.1.4 Lap-Shear Testing Procedure and Parameters

Lap-shear testing was performed by first attaching a 150-kN load cell to the apparatus above the wedge grips. Following this, the bonded assembly was clamped between the wedge grips, as seen below in Figure 4.3. Care was taken to ensure that the grips were tightened on the assembly without straining the sample during the tightening process. Along with this, before beginning the test the wedge grips were inspected to make sure they were square with each other to minimize any bending or twisting strains imparted to the assembly during testing.

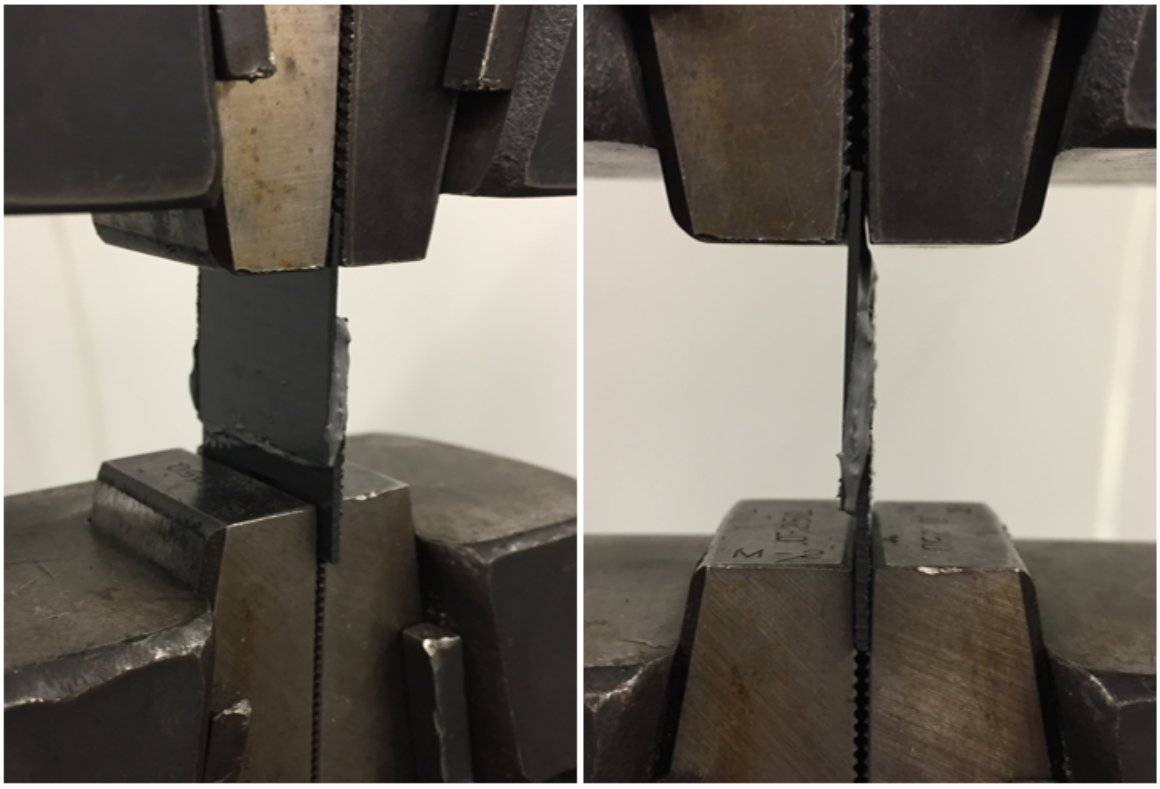

Figure 4.3: Bonded CFRTP assembly clamped into Instron prior to testing.

A program was written in the computer control unit of the Instron to pull the bonded assembly apart at a constant crosshead speed of 1.25 mm/min. The program recorded the sample extension (in mm) and load (in N) every 0.05 seconds during testing until assembly failure occurred. After failure, the recorded data was exported to a Microsoft Excel file to be processed later.

4.2 Lap-Shear Testing of Bonded Assemblies

4.2.1 Description of Experiments

These mechanical testing experiments were performed to correlate the measurements made with the single-probe Kelvin scanner prototype (reported in Chapter 3) with the shear

strength of bonded CFRTP assemblies. Since the motivating work behind this project correlated SP distributions with fracture toughness of bonded assemblies, where narrower distributions (as noted by smaller standard deviations of SP, or larger $1/\sigma_{SP}$ values) measured on plasma-treated CFRTPs had a higher fracture toughness than control assemblies, the following experiments aimed to reproduce these results but correlate them with measurements made by the single-probe Kelvin scanner prototype. Two sets of bonded assemblies were prepared for this test. The first set consisted of twelve control (un-treated) CFRTP coupons bonded into six assemblies. The second set consisted of twenty plasma-treated CFRTP coupons bonded into ten assemblies. The plasma-activated samples were treated using the same procedure discussed in Chapter 3. Pairs of coupons were treated and bonded such that their activated surfaces were the surfaces being bonded together (i.e. the epoxy was applied to the surface-activated sides of the samples). Each pair of plasma-treated coupons used to create an individual assembly was treated at different durations out from bonding. In other words, one pair of samples was treated five days prior to bonding, another pair treated immediately before bonding, and so on. This was done to see if the stability of the activation state, as indicated by the narrow standard deviation of SP measured by the single-probe Kelvin scanner prototype in the days after plasma treatment, could be correlated with mechanical strength of the bonded assemblies.

The lap-shear testing performed on bonded assemblies investigated two types of failures: material failure and adhesive failure. Material failure occurred when the bond strength of the assembly exceeded the strength of the CFRTP material. When this happened, as the load increased past a critical value the wedge grips began tearing apart the CFRTP material and the assembly began slipping out of the grips. When this situation occurred, the "load at failure" value reported was the highest recorded applied load before the assembly began slipping from the wedge grips. On the other hand, adhesive failure occurred when the adhesive peeled off one of the CFRTP surfaces, leaving the CFRTP coupons of the assembly intact. Figure 4.4 below demonstrates what these two types of failures looked like during lap-shear testing of bonded CFRTP assemblies.

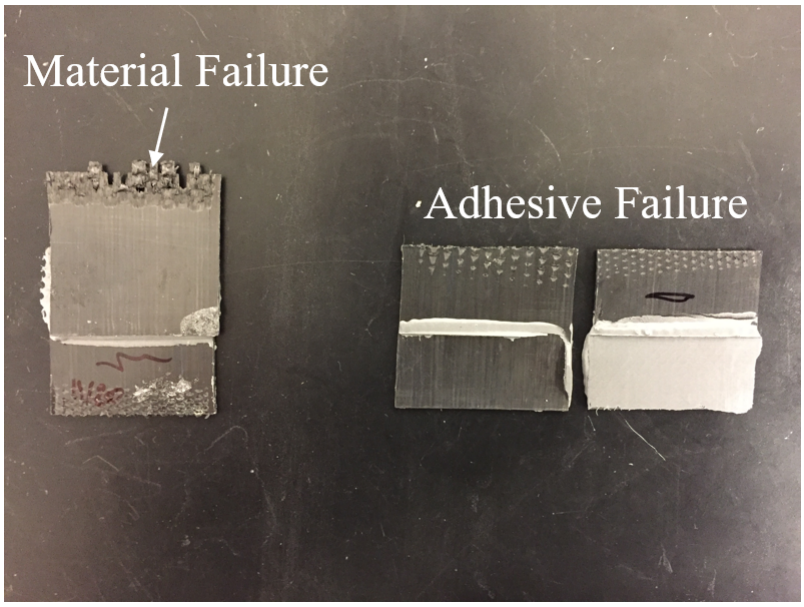

Figure 4.4: Examples of material and adhesive failures from lap-shear testing.

4.2.2 Results

Plasma-treatment of CFRTP samples prior to adhesive bonding increased the bond strength of the resulting epoxy-bonded assembly, as demonstrated by an increased load at failure experienced by plasma-treated assemblies when compared with control, or untreated, assemblies. Furthermore, plasma-treatment increased the probability that an assembly would undergo material failure before undergoing adhesive failure, as 100% of control assemblies underwent adhesive failure while only 20% of plasma-treated assemblies experienced this type of failure.

Out of the 16 total bonded assemblies tested, half of the assemblies experienced adhesive failure while the other half experienced material failure during testing. All six of the control assemblies underwent adhesive failure, whereas eight of the ten plasma-treated assemblies underwent material failure. These results are summarized in Table 4.1 below.

Table 4.1: Failure Mode Count for Tested Bonded Assemblies

Assembly Type	Number of Material Failures	Number of Adhesive Failures
Control	0	6
Plasma-Treated	8	2

Even though 20% of the plasma-treated assemblies underwent adhesive failure while the other 80% of the samples experienced material failure, the fracture toughness as determined by the load measured at failure was similar across all the plasma-treated assemblies. The average load at failure for the plasma-treated assemblies was 8,809 ± 712 N, while the average load at failure for the six control assemblies was 2,635 ± 991 N. Figure 4.5 below demonstrates this three-fold increase in shear bond strength of the plasma-treated assemblies when compared to the control assemblies.

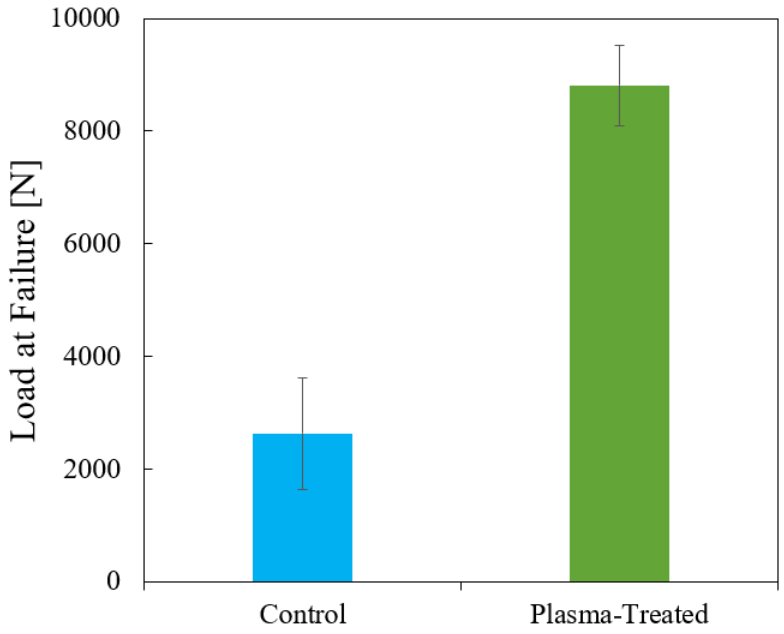

Figure 4.5: Measured load at failure for control and plasma-treated bonded assemblies as determined through lap-shear testing.

4.2.3 Discussion

The results presented above paralleled the motivating results from Chapter 1. Although double cantilever beam testing was performed on the bonded assemblies in the motivating work, the lap-shear testing results presented here confirm that plasma-treatment of CFRTP materials increases the bond strength of the resulting assembly. This is a result of the interfacial interaction between the CFRTP composite material and the epoxy resin used for bonding, which can be discerned by looking at the failure modes of the tested assemblies. Table 4.1 demonstrates that all the control samples tested experienced adhesive failure where the adhesive peeled off the coupon surface, whereas the majority of the plasma-treated assemblies experienced material failure where the adhesive remained in-tact passed the point where the CFRTP coupon failed. This indicates that plasma-treatment creates a favorable surface for the epoxy to bond with, whether it be through physical (etching) or chemical (functionalization or creation of reactive free radicals) means, compared to control or untreated CFRTP coupon surfaces.

Plasma-treated assemblies experienced a load at failure that was over three times larger than the load at failure experienced by control assemblies, with the error bars on the respective values indicating they are statistically different from each other. When comparing the smallest plasma-treated assembly load at failure to the largest control assembly load, there was still a difference of over 3,500 N between the two loads the materials could withstand. The difference between the shear bond strength of plasma-treated and control assemblies may be even larger than what was indicated here, since the bond strength of most of the plasma-treated assemblies was never actually found before the material failed. This result further confirms that plasma-treatment of CFRTP materials significantly increases the bond strength of resulting assemblies compared to control or untreated CFRTP material assemblies.

4.3 Correlation with Single-Probe SP Measurements

These lap-shear tests were performed for two reasons: 1) to recreate the results that motivated this project and 2) to give meaning to the SP measurements made with the single-probe

prototype from the previous chapter. Since the results from lap-shear testing aligned with the double cantilever beam testing performed in the motivating work, correlations with the results reported in Chapter 3 were investigated to understand if the measurements made by the single-probe Kelvin scanner prototype were valuable in predicting desirable properties of the CFRTP materials.

To better understand this relationship between measured SP distribution and shear bond strength of plasma-treated and control materials, the plot shown in Figure 4.6 below was developed. Since the research that motivated this thesis work demonstrated a positive correlation between the inverse standard deviation of the SP measured across a surface ($1/\sigma_{SP}$) and the fracture toughness of bonded assemblies, a similar trend was investigated here. Figure 2.4 therefore plots the load at failure as determined through lap-shear testing as a function of $1/\sigma_{SP}$ for nominally-identical samples. Nominally-identical means the samples were treated under the same conditions and SP measurements were made on one set of samples at the same time out from treatment that bonding occurred for the other set of samples undergoing mechanical testing. In other words, if a sample was plasma-treated and then bonded three days after treatment, a SP measurement was performed by the single-probe prototype on a nominally-identical plasma-treated sample three days after treatment of that sample. The $1/\sigma_{SP}$ values in the plot below were taken from the nominally-identical samples whose standard deviations (σ_{SP}) were reported in Table 3.2. This means that the $1/\sigma_{SP}$ values reported here are the inverse of the σ_{SP} values reported in Table 3.2 averaged over three samples before treatment (control) and in the days succeeding treatment.

For the plasma-treated samples plotted in Figure 4.6, there are two clear regimes present. The single point plotted on the left (with a low $1/\sigma_{SP}$) corresponds to a sample whose SP measurement was performed immediately after plasma-treatment. As mentioned in Chapter 3, the large standard deviation of the SP measurement performed on the CFRTP samples immediately after treatment is most likely due to the dissipation of built up charge (on the surface and in the bulk) from the plasma-treatment process. The second regime corresponds to the samples measured in the days after plasma-treatment (specifically one, two, three, and five days after treatment). These four samples all had a stable SP measurements and similar standard deviations of those measurements across their surfaces. Despite these differences in $1/\sigma_{SP}$ values, the plasma-treated samples are all distinguishable from the control samples when looking at the load at failure measured by lap-shear testing of bonded assemblies.

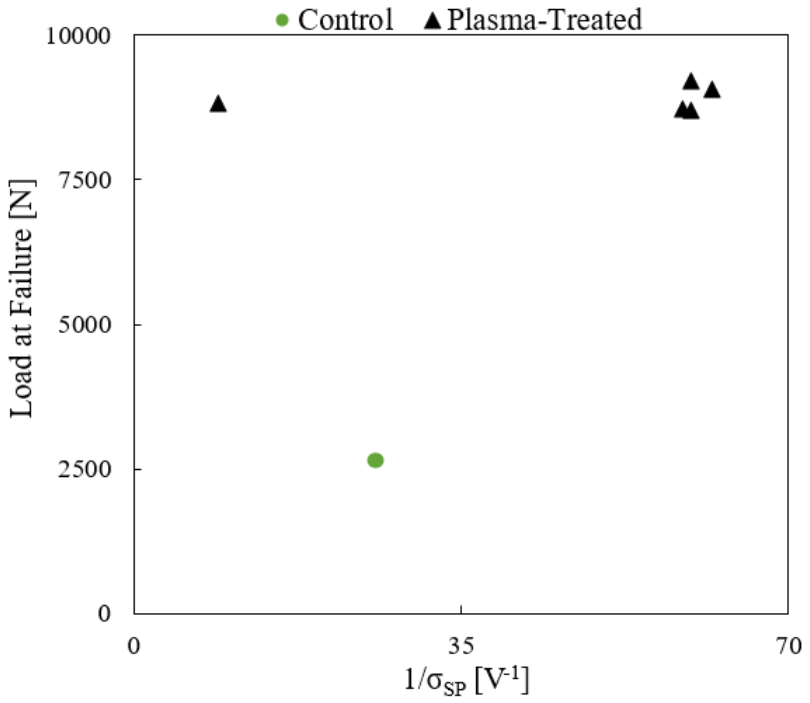

Figure 4.6: Plot of load at failure vs $1/\sigma_{SP}$ values for nominally-identical samples.

A better visualization of this correlation between plasma-treated and control CFRTP coupons can be seen in Figure 4.7 below. On the primary axis of the bar graph, the load at failure is plotted for both control and plasma-treated bonded assemblies (similar to Figure 4.5). On the secondary axis is $1/\sigma_{SP}$ for the nominally-identical plasma-treated samples. The $1/\sigma_{SP}$ measured immediately after plasma-treatment (which was much lower than any other measurements made on the plasma-treated samples) was excluded due to the likelihood that built up charge from the plasma-treatment process interfered with the measurement, leading to the anomaly.

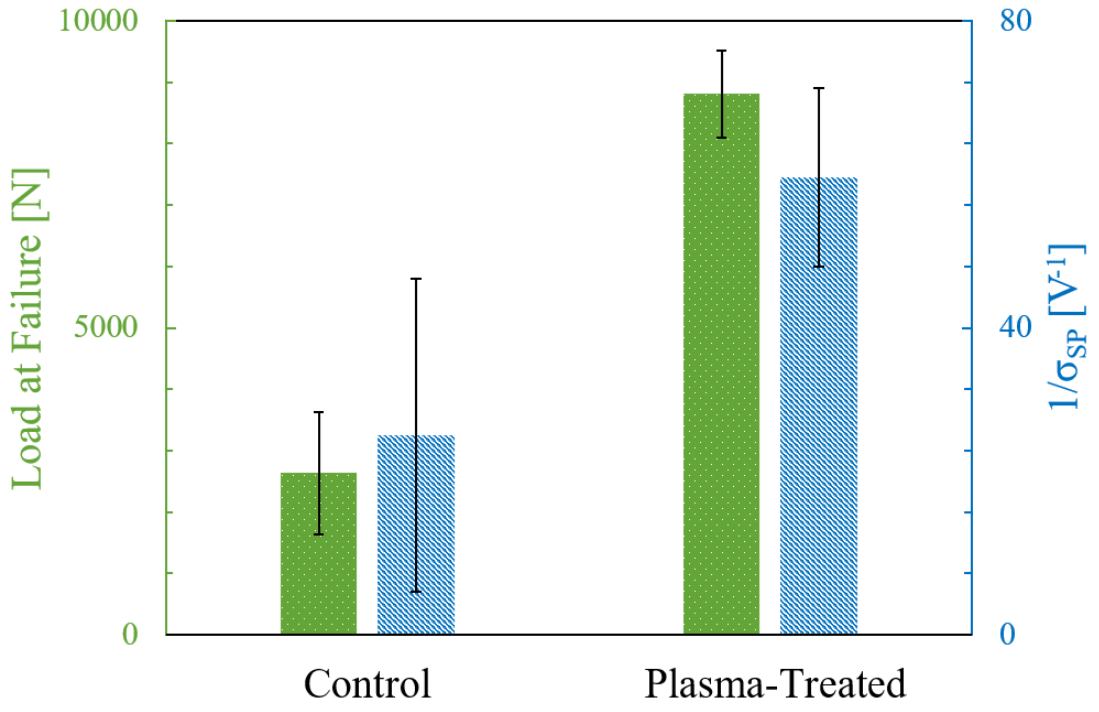

Figure 4.7: Graph of the load at failure and $1/\sigma_{SP}$ values as a function of sample type.

Figure 4.7 demonstrates the parallel between the fracture toughness of bonded CFRTP assemblies (as determined by the measured load at failure from lap-shear testing) and the $1/\sigma_{SP}$ of the SP measurements on plasma-treated and control samples. Although the error bars slightly overlap on the $1/\sigma_{SP}$ values reported, which is likely due to the nonuniformity of control CFRTP materials, there is a strong correlation between $1/\sigma_{SP}$ and fracture toughness. This result gives weight to the measurements reported in Chapter 3, as it indicates that measurements made with the single-probe Kelvin scanner prototype can be indicative of the bond strength of assemblies made from the CFRTP materials. This result legitimatizes the idea that this Kelvin scanner prototype can be used as a basis for quality control of plasma-treated CFRTP materials. Since the prototype Kelvin scanner can work in ambient conditions, is automated, utilizes a non-contact, non-destructive measurement technique, and can predict bond strength of CFRTP assemblies prior to bonding through the measurement of standard deviations of SP across a sample surface, the device shows promise as a quality control instrument for assessing CFRTP materials used in manufacturing. The following chapter discusses experiments aimed at scaling up the single-probe Kelvin scanner

device to rapidly make simultaneous measurements with multiple probes, therefore making the device more suitable for automation and assessment of larger parts (e.g. aircraft wings) that would be of interest to manufacturing.

Chapter 5

Multi-Probe Prototype Testing

The work in this chapter expands upon the work and results discussed in Chapter 3. Although the single-probe Kelvin scanner prototype was able to distinguish between plasma-treated and control CFRTP samples based on comparison of standard deviations of measured SP values across sample surfaces, further improvements still needed to be made in order for the device to meet the needs of the aerospace and automotive industries. Most importantly, the measurement speed and durability need to be drastically improved in order to measure and map larger materials. The single-probe prototype discussed previously could create a SP map of 10 mm x 10 mm, flat CFRTP sample surfaces in just around ten minutes. Although this is beneficial for lab-scale operations, the device as it is presented in Chapter 3 is ill-suited for measuring manufacturing-relevant materials such as aircraft wings, car parts, or implants made of CFRTP composites, whose surfaces are significantly larger and often are not perfectly flat. To meet these quality control needs for surface-activated CFRTP composite materials, the single-probe prototype was therefore scaled up by implementing a multiple-probe design that would allow for the rapid and simultaneous measurement of SP values across larger sample surfaces. The characteristics of these probes and the results from testing the multi-probe Kelvin scanner (MPKS) device are presented below.

5.1 Testing Two-Probe Configuration of Device

5.1.1 Experimental Parameters and Methods

A two-probe configuration was utilized in the following experiments as a proof-of-concept for the use of multiple probes to simultaneously make SP and standard deviation measurements of CFRTP composite material surfaces. The configuration consisted of two stainless-steel probes with tip diameters of 5 mm screwed into an attachment on the end of the extension arm where the single probe was housed in the earlier experiments. The probe centers were around 0.71" away from each other measured from their centerlines. The setup of the two-probe configuration can be seen in Figure 5.1 below.

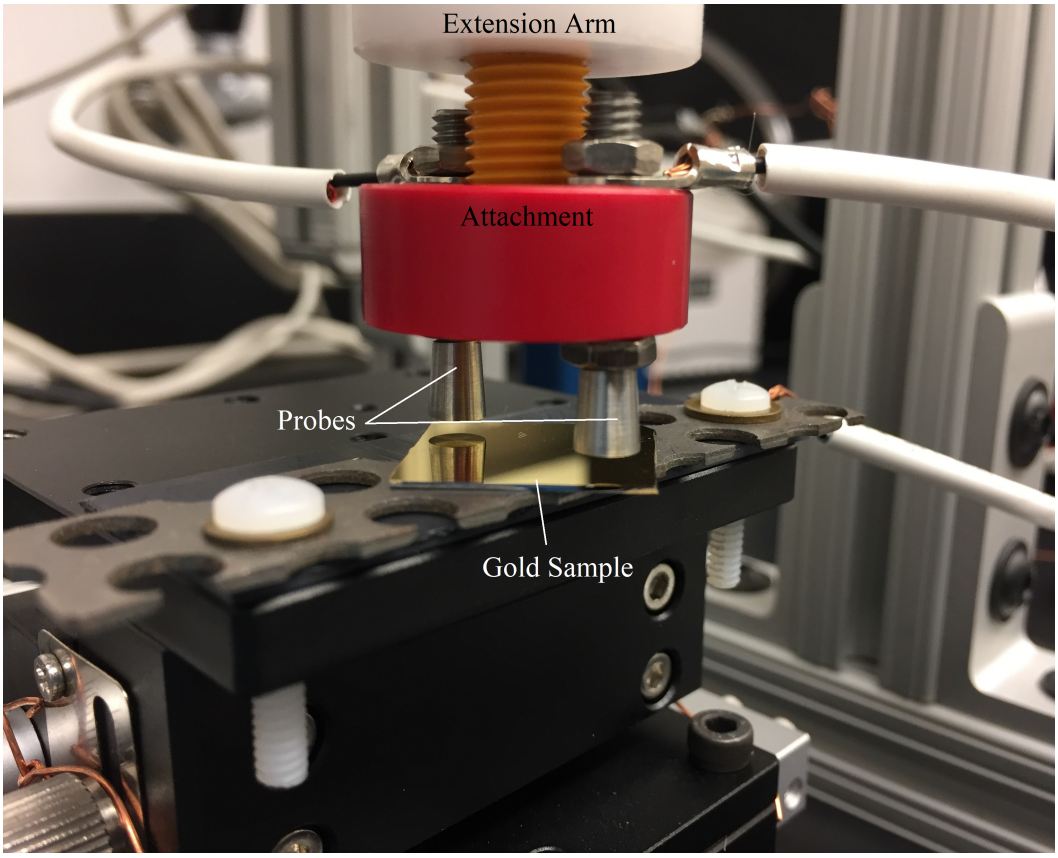

Figure 5.1: Configuration of two-probe setup with respect to a gold sample.

To make SP measurements in the two-probe configuration, a similar practice was used as discussed above with the single probe measurements. The sample was brought in close-enough proximity to the probes such that a change in the output voltage signal could be detected by the probes as a result of their oscillation. For this to be the case, the probes had to have a similar tip-to-sample distance such that they could be simultaneously brought in close-enough proximity to detect this change. This distance was adjusted for each probe by screwing in the probes to a similar height in the arm attachment (as seen above).

Instead of comparing measurements made by one probe to measurements made by the other probe, SP maps of a sample surface were made instead by comparing measurements across the surface by a single probe and finding the average SP and standard deviation of those measurements for the individual probes. Once an SP value and standard deviation (σ_{SP}) were determined for the sample surface for each probe, the standard deviations for each probe were then combined in a root sum squared (RSS) calculation, as seen in equation 5.1. In this equation, i corresponds to each probe and N corresponds to the total number of probes used for the measurement.

$$RSS = \sqrt{\sum_{i=1}^{N} \sigma_{SP,i}^2} \tag{5.1}$$

This analysis was performed to ensure that differences in probe chemistry or composition did not interfere with measurements. Although the probes were both made of the same stainless-steel material, since the Kelvin probe measurement performed here is a surface-sensitive measurement slight differences in probe composition at the tip surface can influence the SP value measured by the probe. This would contribute to an increased standard deviation of SP values measured across the sample surface if the probes were assumed to be identical but in-fact had slightly different compositions. Although it could not be assumed that the probes had identical compositions at their tip surfaces, it could be assumed that the composition of each probe would not change drastically within the ten minute time frame that a given measurement was performed. Therefore, instead of assuming that the probe work functions were identical and comparing the SP values they measure across a sample surface to each other, it was instead assumed that the individual probe work functions were different yet stable for the duration of the measurement so that differences in SP values measured by

the probes could be attributed to true differences in SP of the sample and not differences between the probes.

When reporting the standard deviation of SP across the sample surface for a given measurement using the two-probe configuration, equation 5.1 was used to consolidate the measurements for each probe into a single value to characterize the sample. Since the results presented in Chapter 3 indicated that plasma-treated CFRTP coupons have a smaller standard deviation of their SP than control samples, this trend was expected to continue such that plasma-treated samples would have a smaller RSS value than control or untreated samples when measured with two probes simultaneously.

The experiments discussed below aimed to investigate the MPKS device proposed to determine if it could accurately distinguish between plasma-treated and control CFRTP coupons similar to the single-probe prototype discussed in Chapter 3. The CFRTP materials measured for these tests were unidirectional composites with a PEKK matrix with a thickness of around 0.1 inches. Samples were cut to 1" x 1" or 2" x 1" sizes depending on the tests being performed. The samples were prepared as discussed in Chapter 3, however they were no longer secured to stainless-steel discs due to size limitations and were instead placed directly onto the conducting sample stage when performing measurements. When taking measurements on the samples, four sites were measured by each probe, with each measurement being performed twice to reduce the chance that noise impacted a given measurement at a given site. This resulted in each probe making eight measurements across a given sample surface. An average SP value was determined for each site measured based on the consecutive measurements made on that site. After measuring the four sites, the average SP values found for each site were then averaged together and a standard deviation was found across these values for a given probe. After determining the standard deviation on the SP value for the four sites measured by each probe, equation 5.1 was then used to calculate an RSS value to describe the standard deviation of SP across the entire CFRTP sample surface in order to distinguish between plasma-treated and control samples.

5.1.2 Experiments and Results

The two-probe configuration of the MPKS was able to accurately distinguish between plasma-treated and control CFRTP composites by comparing RSS values for each sample measured over the course of several experiments. The RSS value of plasma-treated CFRTPs was smaller than the RSS value for control samples and often had a smaller error bar than the error on the RSS values for control samples. The two-probe configuration of the MPKS was also able to measure larger samples and similarly distinguish between plasma-treated and control samples, although with larger errors.

The first set of experiments performed with the two-probe MPKS consisted of measuring 1" x 1" control and plasma-treated CFRTP coupons. For a given experiment, four sites were measured by each probe across the sample surface with repeat measurements being made at each site, as mentioned above. The probe-to-sample distance was kept roughly constant for a given measurement by moving the sample stage horizontally underneath the probe without adjusting its height when moving from site-to-site. The sites measured from experiment-to-experiment were held constant. Four experiments were performed over the course of two days, with two experiments being performed on each day. The results from all four experiments were then averaged together to get a representative RSS value for each sample. The results of the measurement of four samples using the two-probe configuration can be seen below in Table 5.1 and Figure 5.2. The plasma-treated sample was stored in controlled relative humidity before treatment, after which it was stored in ambient lab conditions. The Control 1 sample was stored in identical conditions as the plasma-treated sample, while the other two control samples (2 and 3) had been stored in ambient conditions for several weeks prior to measurement.

Table 5.1: Results for Two-Probe Test to Detect Plasma-Treatment on 1" x 1" CFRTPs

Sample	**RSS [V]**	**Error [V]**
Plasma-Treated	0.0141	± 0.0006
Control 1	0.1764	± 0.0616
Control 2	0.0479	± 0.0115
Control 3	0.1280	± 0.0163

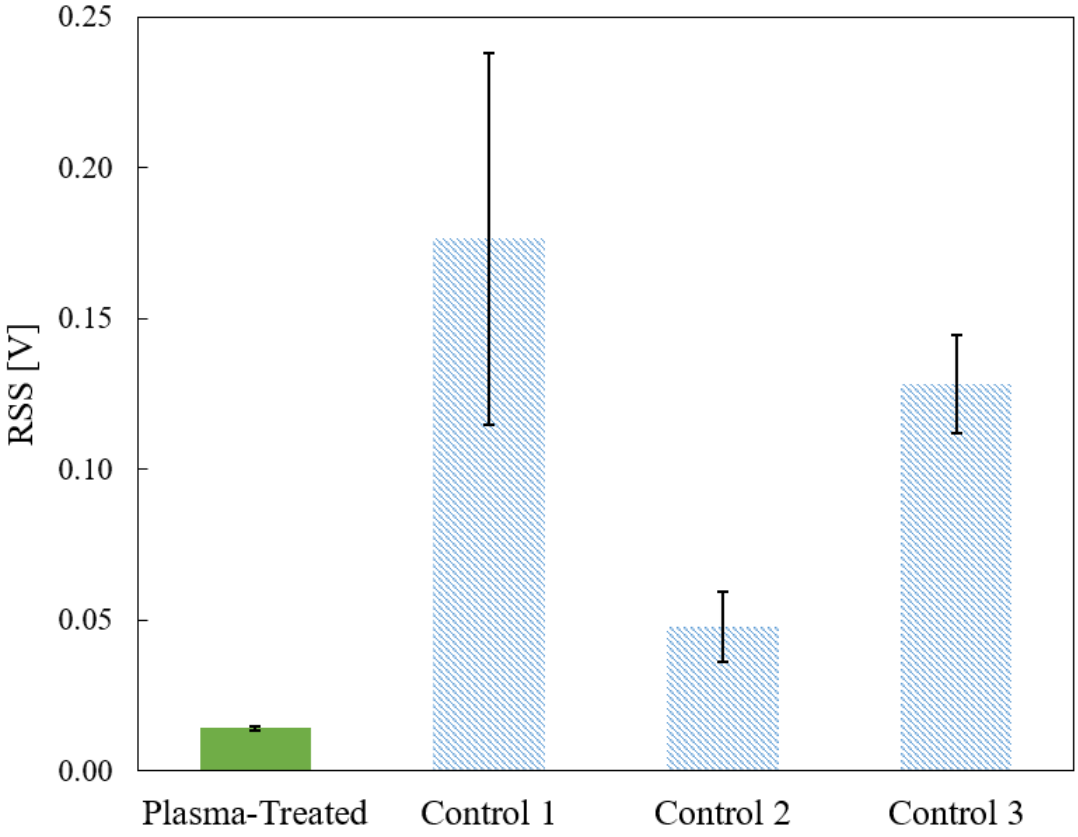

Figure 5.2: RSS values from four measurements on a single plasma-treated CFRTP sample and three control samples.

The RSS value for the plasma-treated sample was significantly lower than the values for all three of the measured control samples. This value was also more well-defined than the control sample values, as determined by over an order of magnitude decrease in error associated with the plasma-treated RSS value compared to the control values.

When measuring these larger samples, the CFRTP coupons were no longer attached to a conductive stainless-steel disc prior to measurement due to size constraints of the disc and the sample stage. Instead, the samples were simply placed on the conducting stage without any extra processing to ensure the carbon fibers were in proper electrical contact with the measurement circuit, as seen in Figure 5.3 below on the left. Because of this difference in sample configuration compared to the original measurements performed in Chapter 3, there

were questions of whether the samples were in proper electrical contact with the rest of the measurement circuit. To resolve this question, an experiment was designed to simulate the sample configuration used for the smaller 10mm x 10mm samples (i.e. securing the samples to a stainless-steel disc with conducting silver paint). This was done by wrapping aluminum foil around the outer edges of the CFRTP sample such that the ends of the exposed carbon fibers were in electrical contact with the aluminum foil and, therefore, the rest of the measurement circuit when placed on the conducting stage.

Several measurements were performed on a 2" x 1" plasma-treated CFRTP surface to probe this question of sample conductivity. Two measurements were performed with aluminum foil wrapped around the edge of the samples, as shown in Figure 5.3 on the right. After this, the aluminum foil was removed from the sample edges and the sample was re-measured in the original configuration (seen on the left in Figure 5.3). Finally, three measurements were performed by grounding the sample on the conducting sample stage for five minutes prior to measurement. This was done by placing the sample on the conducting stage (Figure 5.3 on the left) and grounding the conducting stage surface for 5 minutes, then ungrounding the stage surface and performing the measurement. This measurement was performed three times, each time grounding the stage for five minutes before measurement. Each probe measured three sites across the sample surface for all experiments. The resulting RSS values are shown in Table 5.2 below. The reported RSS value for the first experiment is the average of the two measurements performed with aluminum foil and the reported RSS value for the final experiment is an average of the three measurements performed when grounding the sample prior to measurement.

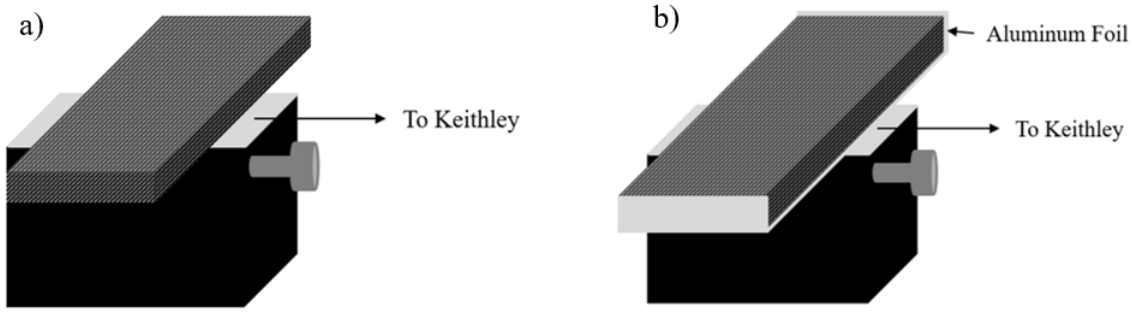

Figure 5.3: Sample configuration on conducting stage (a) and sample configuration with aluminum foil wrapped around the exposed carbon fibers to simulate original sample configuration from Chapter 3 (b).

Table 5.2: Results from Experiments Probing Sample Conductivity

Experiment	**Average RSS [V]**
With Aluminum Foil	0.0100
Immediately After Removing Foil	0.0363
Ground for 5 Minutes Before Measurement	0.0075

The RSS results for the CFRTP when placed on the conducting stage and grounded before measurement paralleled the RSS values for the sample with aluminum foil. When measuring the CFRTP sample immediately after removing the foil, the RSS value increased as a result of each probe reporting larger standard deviations on the measured SP values across the sample surface. Grounding the sample on the sample stage after handling stabilized the RSS values without extra processing needed for the sample to ensure its electrical connectivity to the measurement circuit.

A final set of experiments measuring 2" x 1" CFRTP samples was performed to understand that scalability of the developed instrument. Due to changes made to the sample stage to accommodate the larger sample and non-uniformities associated with the CFRTP surface, the probe-to-sample distance was not kept constant when moving from site-to-site. Instead, the sample stage was lowered to move the CFRTP sample away from the probes, then the stage was moved horizontally so the probes would measure a new site. The stage was then raised back up until the probes were close enough to the sample surface to detect signal

changes induced by probe oscillation, after which a measurement was made. The sample was grounded for ten minutes on the sample stage prior to measurement, then four sites were measured across the sample surface for each experiment. Three experiments were performed over the course of two days, and the average RSS values calculated for each sample are shown below in Figure 5.4.

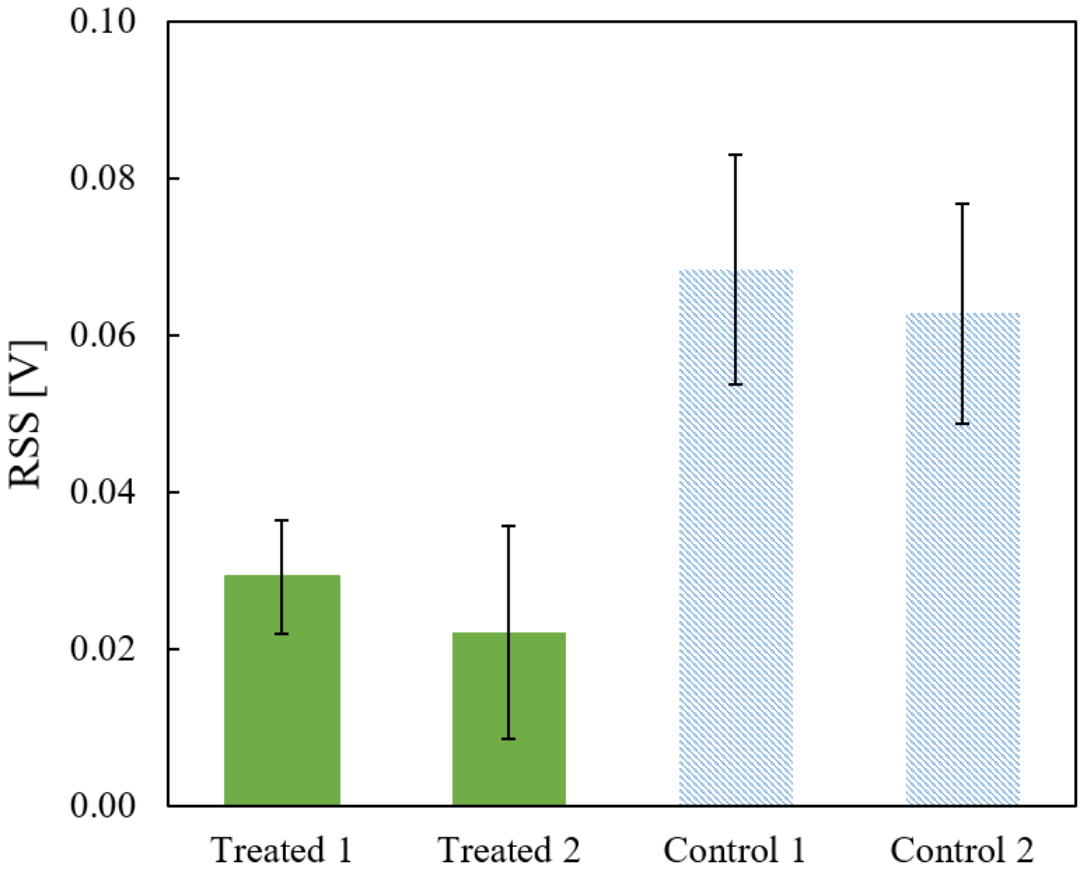

Figure 5.4: RSS results from measuring 2" x 1" plasma-treated and control CFRTP samples with two probes.

5.1.3 Discussion and Conclusions

The first set of experimental results presented above demonstrates that an RSS analysis can be utilized to distinguish between plasma-treated and control CFRTP materials when

performing a multi-probe measurement. The use of two probes, both detecting a narrow standard deviation of SP across their respective measured sites, when measuring the sample surface produces a similar result as what was detected with a single-probe. The RSS value for the plasma-treated sample was both a) smaller (by over an order of magnitude in one situation) than the RSS value calculated for the control samples and b) more well-defined than the control sample values as distinguished by an error that was over a magnitude smaller than the errors of the control samples. This result indicates that the narrow standard deviation on the SP value for plasma-treated samples, detected both in the motivating work and with the single-probe Kelvin scanner results presented in Chapter 3, was also detected by utilizing a dual-probe configuration with the MPKS device. The benefit of this result is that measurement time was drastically improved by this development: whereas it took the single-probe Kelvin scanner around ten minutes to map a 10 mm x 10 mm CFRTP surface, it now takes the same amount of time to measure a surface 1" x 1". This result is a promising indicator that implementing even more probes will further decrease measurement time and allow for the more-rapid assessment of surface-activated materials on a larger scale.

Another promising conclusion from this result has to do with the probe diameter. In the motivating work for this project, the surface defects that resulted in changes in SP were on the order of 10s to 100s of microns. Therefore, a very fine tip had to be used for probing the surface to accurately detect these nonuniformities across the sample surface. When the single-probe Kelvin scanner was developed, there were concerns about spatial averaging of these nonuniformities when implementing a 3-mm tip because of the microscopic size of these defects. However, the 3-mm tip was also able to distinguish between plasma-treated and control CFRTP samples, indicating that the spatial averaging of the measured SP value due to the larger tip size did not significantly interfere with the accuracy of the measurement. This concern was again brought to light when performing the two-probe measurement with the MPKS, since the tip size was again increased, this time to 5 mm. The results from this experiment indicate, however, that plasma-treated and control CFRTP samples can still be distinguished in the current MPKS configuration by comparing RSS values between samples. This result further demonstrates the capacity of this device to be scaled up to rapidly characterize larger surface-activated CFRTP materials.

The results from the experiments probing sample conductivity and configuration shed light on an important anomaly discovered throughout the measurement process dealing with sample

charging. When performing measurements with aluminum foil wrapped around the sample edges, the RSS values were relatively stable, indicating the standard deviations of SP measured by each probe were stable across the two experiments performed. However, upon removing the foil and immediately performing another set of measurements, the RSS value drastically increased. After grounding the sample for five minutes prior to measurement, however, the RSS value returned to similar values as the first experiments. The increase in RSS after handling and subsequent decrease after grounding indicates that significant handling of the material may charge the material surface (or bulk), which will interfere with the resulting measurements if the built-up charge does not have sufficient time to dissipate. When removing the foil, the sample was handled with tweezers and by hand with latex gloves on, so it is likely that built-up static charge on the gloves and in the tweezer was transferred to the sample during this process. Since repetitive grounding of the sample prior to measurement caused the RSS value to continually decrease back to values less than the original measurements, this indicates the importance of grounding samples prior to measurement to improve the stability and reproducibility of the experiments. This result further explains the results discussed in Chapter 3 when performing measurements on CFRTP samples immediately after plasma-treatment. It is likely that the increase in SP and standard deviation measured by the single-probe Kelvin scanner was a result of significant sample charging, as a result of the plasma-treatment process and handling the sample after treatment, that did not have time to dissipate prior to performing measurements. Two important conclusions can therefore be drawn from these experiments. First, grounding the sample prior to performing measurements with the MPKS, especially after significant handling of the sample, is necessary to reduce noise in the measurement and improve measurement accuracy. Second, when measuring these larger 1" x 1" and 2" x 1" samples, no extra processing is required to ensure the sample is in electrical contact with the measurement circuit, as the RSS values reported with and without aluminum foil were similar once the sample had been properly grounded prior to measurement.

The final experiments on the 2" x 1" CFRTP samples demonstrated the ability of the device to measure larger material surfaces. Two-probes could adequately distinguish between plasma-treated and control CFRTP composite surfaces, although the error bars were larger than those that were seen when measuring the smaller samples. This is believed to be due to two issues: 1) changes in probe-to-sample height during a given measurement when moving from site-to-site and 2) errors in the measurement from interference or software malfunction.

The first issue was difficult to control in this setup because of nonuniformities in the modified sample stage and the larger CFRTP samples being measured. The sample stage could not be moved horizontally underneath the probes at a constant height, as it was in the previous experiments, without at least one of the probes contacting the sample surface. Therefore, the probe-to-sample distance had to be reconfigured at each site being measured across the sample surface. If the probe-to-sample distance was different at each site being measured, this could have contributed to differences in the SP measured by each probe and therefore increase the standard deviation of the SP measurement made by each probe across the sample surface. An experiment performed in the following section confirms this idea and conveys the importance of maintaining a constant probe-to-sample distance over the course of a given measurement.

The other potential error was noted when making repeat measurements at each site, which was done for all these experiments to reduce potential errors when measuring. In general, the repeat measurements made on a given site had a standard deviation on the SP value of less than 10 mV, and often times less than 1 mV. However, there were occasions when this error exceeded 10 mV despite the fact that the measurements were made in immediate succession with no changes in the device or probe configuration. On occasion these errors were attributed to a software error, where the measurements made by the probes were flipped (i.e. the measurement made by probe 1 was reported as the measurement made by probe 2 and vice versa), however there were instances where this was not the case and the source of the error could not be determined. This resulted in either having to flip the recorded measurements for each probe (in the case of the software error) or having to exclude or remeasure the site where the error occurred if the source of the error was undetermined. Although these steps were taken to mitigate the impact the errors had on the measurements reported here, these errors still could affect the measurements if care is not taken to understand and analyze the data post-measurement. After these errors were discovered, the measurement program written for data collection was edited to eliminate the chance of a software errors impacting the measurements. After editing the program, no errors were found during measurement with multiple probes (based on the following experiments performed with the four-probe MPKS), so it is believed that the edits made to the software corrected the issue.

5.2 Testing Four-Probe Configuration of Device

5.2.1 Experimental Parameters and Methods

The four-probe configuration of the MPKS looks exactly as it did in Figure 5.1 above except with two more probes added to the attachment on the extension arm. The probes, all with a tip diameter or 5 mm, were configured in the shape of a square with sides of 0.5" in length, as seen in Figure 5.5 below. Adjacent probes were 0.5" apart from each other measured from their centerlines and probes opposite of each other were 0.71" away from each other. The probes were screwed into the attachment such that their tips were roughly parallel with each other, however it was difficult to make the probes perfectly flush because they were all adjusted by hand and held tightly in place with two screws.

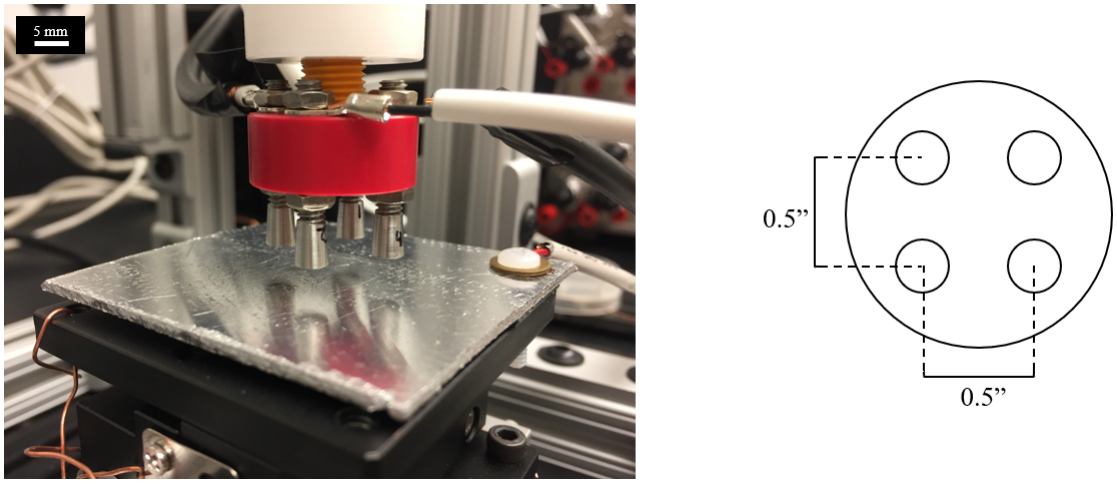

Figure 5.5: Image of four-probe configuration of MPKS and the conducting stage (left) with diagram of probe orientation (right).

5.2.2 Procedure

The same 2" x 1" CFRTP plasma-treated and control samples used in the two-probe experiments discussed above were measured using the four-probe configuration of the MPKS. The sample to be measured was placed on the conducting sample stage and grounded for ten

minutes prior to any measurement. Two sites were measured by each probe on the sample, with repeat measurements being made at each site. This was done by raising the height of the sample stage until each probe was able to detect a signal change as a result of the probe's oscillation. Once each probe could detect a signal change at its respective site, duplicate measurements were made by the probes. The sample stage was then lowered and moved horizontally so that the probes could each measure a new site. The same procedure was then repeated. This resulted in each probe measuring two sites, with repeat measurements at each site resulting in four total measurements made by each probe. The standard deviation of the SP measured by each probe across the sample surface was then calculated and an RSS value was calculated to represent the entire sample in the same way that was discussed in the section above.

5.2.3 Results

The four-probe configuration of the MPKS similarly reported smaller RSS values for plasma-treated CFRTP samples compared with control samples. Measurement time was further reduced by sampling fewer sites on the CFRTP surface. Varying probe-to-sample distance by 30 microns across a set of measurements resulted in a change in SP on the order of almost 90 mV (in the worst case scenario), indicating the importance of keeping this variable constant throughout a measurement.

The first set of experiments involved measuring the two plasma-treated and two control 2" x 1" CFRTP samples that were used previously in the two-probe configuration. Three experiments were performed over the course of two days when measuring these samples, and an average RSS value was calculated for each of the measured samples. The results are shown below in Figure 5.6. The two plasma-treated samples had a smaller average RSS value than the two control samples, although the error bars on those values all overlapped.

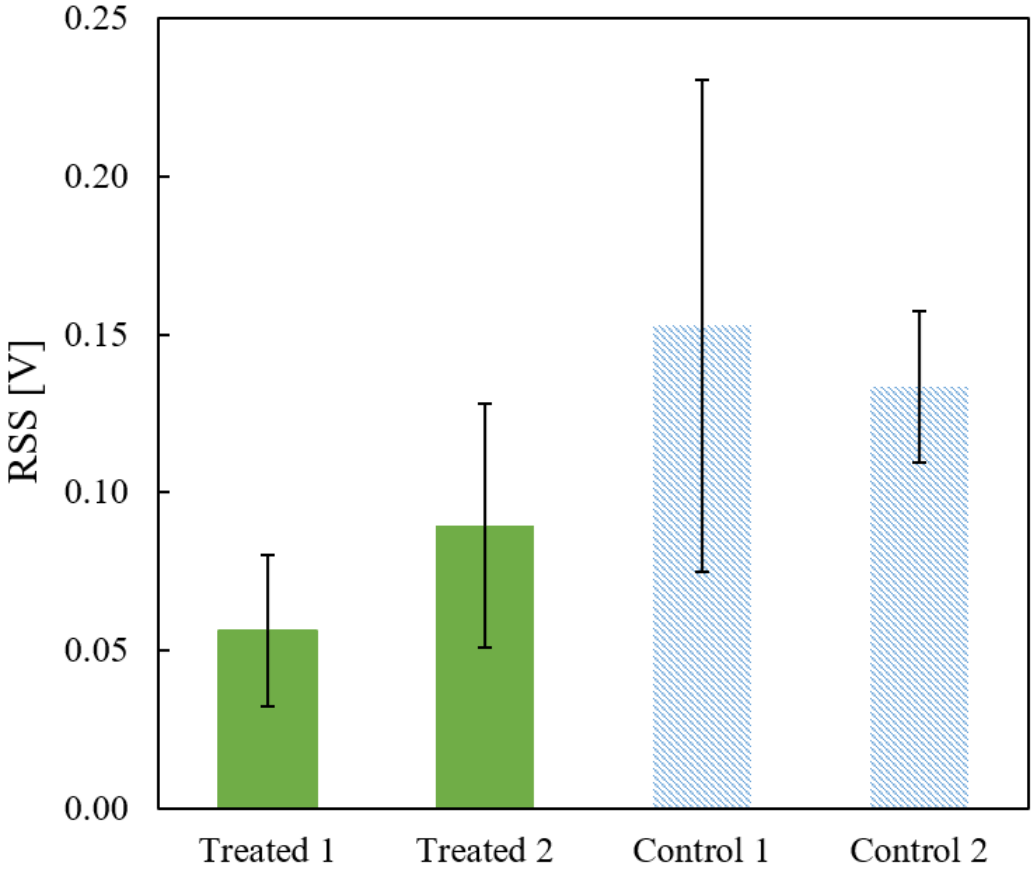

Figure 5.6: RSS results from measuring 2" x 1" plasma-treated and control CFRTP samples with four probes.

The final set of experiments aimed at understanding the impact that changes in probe-to-sample distance during an experiment had on the SP value measured by a given probe. This was done by choosing a site for the probes to measure and making an initial SP measurement. This point was termed the "Zero Point," as seen in Figure 5.7 below. After this, the sample stage was raised or lowered in 10-micron intervals. A measurement was made at each new probe-to-sample distance until four total measurements were made, corresponding to a 30-micron range of probe-to-sample distances. An SP range was then determined for each probe based on the maximum and minimum SP value measured by the probe. This experiment was performed on one of the 2" x 1" control and plasma-treated samples mentioned above and was repeated on consecutive days. The SP ranges calculated for each experiment, sample,

and probe are reported in Table 5.3 below, where Experiment 1 was performed on the first day and Experiment 2 was performed on the second day.

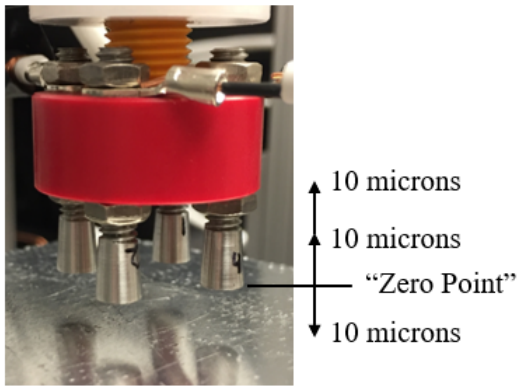

Figure 5.7: Varying probe-to-sample distance over the course of an experiment. An initial SP measurement was made at the "Zero Point", then SP measurements were made at each 10-micron change in probe-to-sample distance.

Table 5.3: Range of SP Values for Each Probe When Varying Probe-to-Sample Distance

Exp.	**Sample**	SP_{P1} **Range** [**V**]	SP_{P2} **Range** [**V**]	SP_{P3} **Range** [**V**]	SP_{P4} **Range** [**V**]
1	Control	0.0172	0.0705	0.0888	0.0898
1	Treated	0.0112	0.0397	0.0595	0.0553
2	Control	0.0120	0.0232	0.0451	0.0404
2	Treated	0.0154	0.0177	0.0527	0.0343

In the worst-case scenario, the SP value measured by a given probe changed by almost 90 mV over a 30-micron change in probe-to-sample distance when measuring a constant site on the sample surface. In other words, the SP value measured when the probe was furthest away from the sample surface was 90 mV different from the value measured when the probe was closest to the sample surface. The SP value measured by a given probe changed by 10s of mV for very probe across a 30-micron change in probe-to-sample distance.

5.2.4 Discussion and Conclusions

The results from the first experiment indicate that the four-probe configuration of the MPKS can also distinguish between plasma-treated and control CFRTP composite materials by comparison of RSS values calculated based on the standard deviation of SP measurements made by each probe. The two plasma-treated CFRTP surfaces had a smaller RSS value than the two control CFRTP surfaces. The error bars on these values, however, did overlap. This indicates that the measurement was not as well-defined as it was with the two-probe configuration as shown in Figure 5.2. This is likely due to two variables: First, in the four-probe configuration of the MPKS, only two sites were measured on each sample as opposed to the four sites measured in the two-probe configuration. The decrease in number of sites would exacerbate the effect that nonuniformities in the SP measured by each probe would have on the resulting RSS value. Assuming a sample has a relatively consistent SP value, then the more sites measured on the sample surface the smaller the standard deviation on the measured SP should be as the average SP determined by a probe would converge to a single value. Therefore, measuring more sites on the CFRTP surface in the four-probe configuration should decrease the calculated RSS value for the surface by reducing the standard deviation of SP reported by a given probe. This effect would be most-apparent on the plasma-treated CFRTP samples, where the SP is more uniform than the control samples.

The second variable that likely contributed to the large errors on the RSS values was differences in the probe-to-sample distance between sites measured by a given probe. Since the sample had to be lowered away from the probes when moving between sites, it was difficult to ensure that the probe-to-sample distances were similar for a given probe when comparing between measurement sites on a sample. The second set of experiments, which systematically varied the probe-to-sample distance throughout an experiment, shed light on the impact that these variations in distance had on the measured SP of the sample surface. At a given location, the SP measured by a probe could vary anywhere from 10-90 mV over a 30-micron span of probe-to-sample distances. This indicates that, when scanning from site-to-site across a sample surface, if the probe-to-sample distance is not kept constant for a given probe then there could be large variations in the SP value measured by the probe. Upon further research, it was found that these effects have been studied and can be minimized through rigorous sheilding and vibration-dampening practices [9, 13], however this noise is difficult to get rid of completely. It therefore becomes difficult to deconvolute the

effects of changing probe-to-sample distance from the effects of plasma-treatment on a given surface, since a plasma-treated sample could have a large standard deviation of its SP measured across its surface if the probe-to-sample distance varied significantly when measuring different sites on the surface. This result supports the idea that changes in probe-to-sample distance when making measurements with the four-probe MPKS likely contributed to the large error bars seen in the resulting RSS values calculated for plasma-treated and control CFRTP samples.

Overall, the four-probe configuration of the MPKS device measured a smaller RSS value for plasma-treated CFRTP samples than control samples, which paralleled the measurements made in the two-probe configuration. These measurements, however, were much noisier than the measurements made with two probes, which was likely a result of a decrease in the number of measurement sites and changes in the probe-to-sample distance when moving from site-to-site. To improve upon the four-probe measurements reported here, a more-robust probe head should be developed such that the probe tips are all parallel and flush with each other and can thus scan across a flat sample surface while maintaining a constant probe-to-sample distance. Keeping this distance constant when making measurements across a sample surface should remove a confounding variable from the SP measurement, making the measurements more accurate and dependable when assessing the surface activation state of CFRTP materials.

5.3 Future Work

Future work revolves around improving the signal-to-noise ratio and further developing the multi-probe aspect of the Kelvin scanner device presented above. Although the signal-to-noise ratio has been improved drastically over the course of this thesis work by implementing shielding methods, using anti-vibration equipment, and trying to reduce sources of interference, there is still more work to be done to prepare this instrument for successful operation in a manufacturing environment where there is not the same level of environmental control as can be found in a laboratory setting.

The multi-probe aspect of this device also serves as a focal point for future development. The two-probe configuration of the MPKS has proven successful in distinguishing between

plasma-treated and control CFRTP coupons, therefore serving as a proof-of-concept for the further development of the device. The four-probe configuration also demonstrated the ability to distinguish between control and plasma-treated materials, however the RSS values were not as well-defined as they were in previous configurations. A better understanding of the probe-sample interaction, as it relates to probe diameter, probe-to-sample distances, and differences between probes when making a simultaneous measurement, needs to be developed to improve the precision and accuracy of measurements and further demonstrate the efficacy of the MPKS device.

Implementing more probes for simultaneous assessment of surface activation of CFRTP composites is a necessity to speed up measurement time and allow for the assessment of surfaces that are significantly larger than those measured in this project. Further developing this aspect of the MPKS would allow the device to transition from a laboratory-scale instrument to a manufacturing-ready quality control device for assessing surface activation states of CFRTP materials, from aircraft wings to biomedical implants, used in various industries.

Chapter 6

Summary and Conclusions

To meet the quality control needs of manufacturing industries utilizing surface-activated CFRTP materials, an instrument utilizing a non-destructive measurement technique was developed in this thesis. The device, which operates like a Kelvin probe, makes no contact with the CFRTP surface during measurement (which could be destructive to the material or its activation state), can operate in ambient conditions, and can reliably make measurements in loud laboratory environments. These qualities make the device a suitable candidate for manufacturing environments where ruggedized yet robust instruments that can assess the activation state of composite materials in a wide variety of conditions are needed.

This novel instrument takes advantage of a recent discovery in KPFM related to plasma-treated composite materials, assessing the activation state of the material by measuring the uniformity of the activation state across the material surface. This uniformity was determined by measuring the SP distribution across the surface of the sample with a prototype Kelvin scanner device. The standard deviation of the SP measured across the CFRTP surface was correlated with control and plasma-treated samples, where narrow standard deviations (i.e. smaller values) were representative of plasma-treated samples and broad standard deviations (i.e. larger values) were representative of control samples. These results were reproduced through several experiments utilizing the single-probe Kelvin scanner prototype, including a blind test of three CFRTP samples as well as several experiments of varying timescales probing CFRTP material surfaces. The prototype device, in a single-probe configuration, was able to reproducibly distinguish between control and plasma-treated CFRTP materials through comparisons of standard deviations of the SP distributions across the sample surfaces it measured.

To further establish the efficacy of the measurements made by the single-probe device, mechanical testing in the form of lap-shear testing was performed on epoxy-bonded CFRTP assemblies. Sets of plasma-treated and control samples were bonded with epoxy under identical procedures and then pulled apart using a universal testing apparatus, measuring the load at which each assembly failed, either through material failure or adhesive failure. Conclusions of the lap-shear testing indicated that plasma-treatment of CFRTP samples before bonding increased the shear bond strength of the resulting assembly by threefold compared to control, or untreated, bonded assemblies. The control samples were also more likely to undergo adhesive failure as opposed to the plasma-treated assemblies, which were more likely to experience material failure. This indicated that 1) the shear bond strength of the plasma-treated assemblies may have been even higher than what was recorded had the material been able to withstand a larger load and 2) the plasma-treatment of the CFRTP surfaces created a stronger interface between the material and the epoxy. When correlated with measurements made by the single-probe Kelvin scanner prototype, the shear bond strength of epoxy-bonded CFRTP assemblies was inversely related to the standard deviation of SP across the sample surface. In other words, one could use the prototype Kelvin scanner device to measure the standard deviation of the SP across a CFRTP material surface and predict the resulting shear bond strength of an epoxy-bonded assembly made from that material, where a narrow standard deviation of SP would predict a strong bond and broad standard deviation would predict a weak bond.

To better prepare the device for manufacturing environments, where automation would be required and materials significantly larger than the samples measured here would need to be assessed, the single-probe prototype was scaled up into a multi-probe Kelvin scanner device, or MPKS. This configuration involved the exact same device as discussed earlier except with multiple probes implemented to simultaneously make measurements in parallel on larger surfaces. The configurations included a two- and four-probe setup with a tip diameter that was 2-mm larger than what was used in the single-probe configuration. This was done to improve the speed at which larger surfaces and materials could be measured. To make measurements in this configuration, each probe measured an SP distribution across a sample surface and the standard deviations of the SP measured by each probe were combined into a single value using a root sum squared (RSS) calculation. This allowed for the use of the same measurement principle as the single-probe prototype device while excluding potential effects that probe differences (e.g. composition or probe-to-sample distance) had on the resulting

measurement. Using this calculation, plasma-treated and control CFRTP sample surfaces could be distinguished by comparison of RSS values for each sample, with smaller RSS values corresponding to plasma-treated samples and larger RSS values corresponding to control samples. The implementation of multiple probes allowed for an increased measurement speed from the single-probe configuration: whereas the single-probe prototype could measure a 10mm x 10mm sample in around ten minutes, the four-probe configuration could measure a 2" x 1" sample in less than five minutes. Although this increase in measurement speed came with a decrease in precision of the measurement, further improvements in device design and an improved understanding of the multi-probe configuration, especially as it relates to changes in probe-to-sample distance, will increase the accuracy of the measurement process and prepare this device for operation in manufacturing-relevant environments.

In conclusion, the MPKS device developed throughout this work serves as a promising tool for assessing the surface-activation state of plasma-treated CFRTP materials. The non-contact, non-destructive device can operate in ambient conditions and determine differences between plasma-treated and control CFRTP composite samples through comparison of the standard deviation of SP values measured across a sample surface. Correlating measurements made by the device with the shear bond strength of epoxy-bonded CFRTP assemblies further demonstrated the advantage this device has in being able to predict bond strength through non-destructive means before bonding is performed. This quality control device has begun the preliminary stages of scale-up, as steps were taken to automate the device and increase its signal-to-noise ratio and measurement speed. Implementing multiple probes to simultaneously measure activation states across a sample surface further improved measurement time and demonstrated the ability to measure larger CFRTP surfaces without losing the ability to distinguish between plasma-treated and untreated CFRTP materials.

References

[1] Baikie, I. D., E. Venderbosch, J. A. Meyer, and P. J. Z. Estrup. "Analysis of stray capacitance in the Kelvin method." *Review of scientific instruments* 62, no. 3 (1991): 725-735.

[2] Baikie, I. D., and P. J. Estrup. "Low cost PC based scanning Kelvin probe." *Review of scientific instruments* 69, no. 11 (1998): 3902-3907.

[3] Baikie, I. D., S. Mackenzie, P. J. Z. Estrup, and J. A. Meyer. "Noise and the Kelvin method." *Review of scientific instruments* 62, no. 5 (1991): 1326-1332.

[4] Bazaka, Kateryna, Mohan V. Jacob, Russell J. Crawford, and Elena P. Ivanova. "Plasma-assisted surface modification of organic biopolymers to prevent bacterial attachment." *Acta biomaterialia 7*, no. 5 (2011): 2015-2028.

[5] Costa, Anahi Pereira da, Edson Cocchieri Botelho, Michelle Leali Costa, Nilson Eiji Narita, and José Ricardo Tarpani. "A review of welding technologies for thermoplastic composites in aerospace applications." *Journal of Aerospace Technology and Management* 4, no. 3 (2012): 255-265.

[6] Favaloro, Michael. "A Comparison of the environmental attributes of thermoplastic vs. thermoset composites. *Cell* 978 (2009): 270-6011.

[7] Gomathi, N., A. Sureshkumar, and Sudarsan Neogi. "RF plasma-treated polymers for biomedical applications." *Current science*, (2008): 1478-1486.

[8] Hale, Justin. "Boeing 787 from the Ground Up." *AERO Magazine* Qtr_04.06, 2017.

[9] Liscio, Andrea, Vincenzo Palermo, Klaus Müllen, and Paolo Samorì. "Tip - sample interactions in Kelvin probe force microscopy: quantitative measurement of the local surface potential." *The Journal of Physical Chemistry C* 112, no. 44 (2008): 17368-17377.

[10] Katnam, K. B., L. F. M. Da Silva, and T. M. Young. "Bonded repair of composite aircraft structures: A review of scientific challenges and opportunities." *Progress in Aerospace Sciences* 61, (2013): 26-42.

[11] Offringa, Arnt R. "Thermoplastic composites - rapid processing applications." *Composites Part A: Applied Science and Manufacturing* 27, no. 4 (1996): 329-336.

[12] Oldham, T., D. R. Ferriell, M. A. Belcher, A. Rubin, and E. Thimsen. "Highly Uniform Activation of Carbon Fiber Reinforced Thermoplastics by Low Temperature Plasma." *ACS Appl Polym Mater* In Review.

[13] Rossi, Frank. "Contact potential measurement: Spacing-dependence errors." *Review of scientific instruments* 63, no. 9 (1992): 4174-4181.

[14] Rouchon, Jean. "Certification of large airplane composite structures." In *ICAS Congress Proceedings*, vol. 2, pp. 1439-1447. 1990.

[15] Shen, Chi-Hung, and George S. Springer. "Effects of moisture and temperature on the tensile strength of composite materials." *Journal of Composite Materials* 11, no. 1 (1977): 2-16.

[16] Slepička, P., N. Slepčková Kasálková, E. Stránská, L. Bačáková, and V. Švorčík. "Surface characterization of plasma treated polymers for applications as biocompatible carriers." *Express Polymer Letters* 7, no. 6 (2013).

[17] Soutis, Costas. "Carbon fiber reinforced plastics in aircraft construction." *Materials Science and Engineering: A* 412, no. 1-2 (2005): 171-176.

[18] Soutis, C. "Fibre reinforced composites in aircraft construction." *Progress in aerospace sciences* 41, no. 2 (2005): 143-151.

[19] Wingfield, J. R. J. "Treatment of composite surfaces for adhesive bonding." *International journal of adhesion and adhesives* 13, no. 3 (1993): 151-156.

[20] Yamazaki, Kumiko, Taiji Yakushiji, and Kiyotaka Sakai. "Nanoscale analysis of hydrophilicity–hydrophobicity distribution on inner surfaces of wet dialysis membranes by atomic force microscopy." *Journal of membrane science* 396 (2012): 38-42.

[21] Yasuda, T., T. Okuno, and H. Yasuda. "Contact angle of water on polymer surfaces." *Langmuir* 10, no. 7 (1994): 2435-2439.

[22] Zaldivar, R. J., H. I. Kim, G. L. Steckel, J. P. Nokes, and B. A. Morgan. "Effect of processing parameter changes on the adhesion of plasma-treated carbon fiber reinforced epoxy composites." *Journal of Composite Materials* 44, no. 12 (2010): 1435-1453.

[23] Zaldivar, R. J., H. I. Kim, G. L. Steckel, D. Patel, B. A. Morgan, and J. P. Nokes. "Surface preparation for adhesive bonding of polycyanurate-based fiber-reinforced composites using atmospheric plasma treatment." *Journal of Applied Polymer Science* 120, no. 2 (2011): 921-931.

[24] Zaldivar, R. J., J. Nokes, G. L. Steckel, H. I. Kim, and B. A. Morgan. "The effect of atmospheric plasma treatment on the chemistry, morphology and resultant bonding behavior of a pan-based carbon fiber-reinforced epoxy composite." *Journal of composite materials* 44, no. 2 (2010): 137-156.

Novel Device for Characterization of Surface-Activated CFRTPs, Simon, M.S. 2019